Statistical Properties of Avalanches on Complex Networks

by

M. Y. Carpenter

B.S., University of Colorado-Boulder, 2012

A thesis submitted to the

Faculty of the Graduate School of the

University of Colorado in partial fulfillment

of the requirements for the degree of

Master of Science

Department of Applied Mathematics

2012

This thesis entitled:
Statistical Properties of Avalanches on Complex Networks
written by M. Y. Carpenter
has been approved for the Department of Applied Mathematics

_____

Prof. Juan G. Restrepo

_____

Prof. Jem Corcoran

_____

Prof. Anne Dougherty

Date _____

The final copy of this thesis has been examined by the signatories, and we find that both the content and the form meet acceptable presentation standards of scholarly work in the above mentioned discipline.

Carpenter, M. Y. (M.S., Applied Mathematics)

Statistical Properties of Avalanches on Complex Networks

Thesis directed by Prof. Juan G. Restrepo

We characterize the distribution of sizes and durations of avalanches propagating in complex networks. We find that the statistics of avalanches can be characterized in terms of the Perron-Frobenius eigenvalue and eigenvectors of an appropriate adjacency matrix which encodes the structure of the network. By using mean-field analyses, previous studies of avalanches in networks have not considered the effect of network structure on the distribution of size and duration of avalanches in all cases. Our results are specific to individual networks and allow us to find expressions for the distribution of size and duration of avalanches starting at particular nodes. These findings apply more broadly to branching processes in networks such as cascading power grid failures and critical brain dynamics. In particular, our results show that some experimental signatures of critical brain dynamics (i.e., power-law distributions of neuronal avalanches sizes and durations), are robust to complex underlying network topologies.

We model avalanches in complex networks by considering a collection of connected nodes where the connection strength between two nodes determines the probability that an excitation is passed from one node to the next. Networks of size N can be identified with a $N \times N$ adjacency matrix where the ij^{th} entry represents the connection strength from node i to node j. Networks are separated into three classes: subcritical, critical, and supercritical based on the largest eigenvalue of the adjacency matrix. We are able to determine the distribution for avalanche size and duration for each type of network.

Dedication

To my mother, my father, my sister, and my friends, for not only putting up with my eccentricity, but encouraging and supporting it.

Acknowledgements

This thesis would not have been possible without the tireless efforts of Professor Juan G. Restrepo for not only serving as my thesis advisor, but also for encouraging me and challenging me in the classroom and in my research. He, as well as Daniel Larremore, have worked to guide me through this dissertation and on to a successful future.

I would also like to extend my thanks to my thesis committee including Professor Juan Restrepo, Professor Jem Corcoran, and Professor Anne Dougherty for donating their time and effort into helping my endeavor.

I would like a special thanks for my friends and family who supported me through my struggles and encouraged me to continue my work despite the hardships, especially to Keegan Boyle and Levi Cai for helping me revise and rewrite my thesis.

Research was made possible thanks to NSF MCTP Grant No DMS-0602284.

Contents

Chapter

1 Introduction 1

1.1 Formulation 2

1.1.1 Adjacency Matrix 3

1.1.2 Degree Distributions 4

1.1.3 Degree Correlations 6

1.2 Model Used in This Thesis 7

2 Distribution of Avalanche Duration 13

2.1 Subcritical Networks ($\lambda < 1$) 16

2.2 Supercritical networks ($\lambda > 1$) 18

2.3 Critical Networks ($\lambda = 1$) 21

2.4 Numerical Verification 23

3 Distribution of Avalanche Sizes 31

3.1 "Brute Force" Method 33

3.2 Inverting The Laplace Transform 37

3.3 Numerical Verification 40

4 Discussion 44

Bibliography 46

Figures

Figure

1.1 An Example Adjacency Matrix 3

1.2 Degree Correlations 8

1.3 Example Avalanche 11

2.1 Numerically Testing b_n Prediction 15

2.2 Histograms of Avalanche Duration 24

2.3 Numerically Testing Exponential Decay Rates 25

2.4 Compairing Out-Degree and Eigenvalue Entry 30

3.1 Histograms of Avalanche Size 38

3.2 Numerically Testing Avalanche Size Prediction 42

3.3 Numerical Results from Biological Applications 43

Chapter 1

Introduction

Networks are composed of individual components which can be linked together in a variety of ways. These can be humans interacting in a social network, computers passing data across the world wide web, animals predating on other animals in the food web, power plants supplying energy to bustling cities, or neurons transmitting electric signals giving you the cognitive ability to read this thesis. Rather than study each individual component,l human, computer, or neuron, we study the whole: this thesis is dedicated not to the study of individual components, but to the study of networks, and the interactions and connections within.

The study of avalanches of activity in complex networks is relevant to a diversity of fields, including epidemiology, geneology, and neuroscience. The simplest case of an avalanche corresponds to a branching process, which was studied first by Galton and Watson [1] and whose generalizations have been studied for many decades [2, 3]. These branching processes can be considered as avalanches propagating in a tree network, and generalizations where avalanches propagate in a more general network have been considered: self-organized criticality in the "sandpile" model [4], and the related topic of critical percolation exponents [5] have been studied on complex networks. Others have investigated avalanches on networks, characterizing the expected size of cascades in clustered random networks under a variety of dynamics [6], as well as characterizing distributions of unordered binary avalanches via "exhaustive percolation" on random networks [7], on networks with arbitrary degree distribution [8], and in random and all-to-all networks of spiking neurons [9].

Although the work in this thesis can be applied to many situations, we first consider an excitable

neural network. When a neuron fires, it stimulates other neurons which may subsequently fire, and when this linked activity occurs in a cascade, it is called a *neuronal avalanche*. Recent experiments have studied neuronal avalanches of activity in the brains of awake monkeys [10] and slices of rat cortex [11], and found that when the tissue is allowed to grow and operate undisturbed in homeostasis [12], both the size and temporal duration of neuronal avalanches is distributed according to a power-law. In contrast, the application of drugs that selectively decrease the activity of inhibitory or excitatory neurons results in avalanches with different statistics [11]. It has therefore been argued theoretically and demonstrated experimentally, that many neuronal networks operate in a critical regime that leads to power-law avalanche distributions [11], maximized dynamic range [11, 13, 14, 15], and maximized information capacity [16, 17, 18]. Therefore, it is of great interest to characterize the critical state and to understand how the experimental signatures of criticality may change upon modifications to the underlying network (e.g., those induced by the drugs used in the experiment).

1.1 Formulation

Formally, we define a network as a system with N nodes and M links between the nodes, where each link is an ordered pair of nodes (n, m) indicating a link from node n to node m. If the links do not have a specific direction the network is said to be *undirected* (e.g., adding a friend on facebook requires that they add you back). We can view undirected links as an unordered pair, but we will instead view undirected networks as a subset of *directed* networks where there is a directed link going both ways between nodes. A network is said to be *simple* if there are no self-connections (a link from node m to node m) and no multiple-connections (more than one link from node p to node q). A network is said to be *complex* if there are non-trivial topological features (e.g., a ring or a lattice would not be complex). When we assume a network is complex, so we are assuming there is no underlying order and the connections are sufficiently random to mimic a social or biological network. We are interested in simple (in the sense defined above), complex networks for their biological, social, and engineering applications.

1.1.1 Adjacency Matrix

It is convenient to represent these networks as a $N \times N$ matrix adjacency matrix. We will define the adjacency matrix to be the $N \times N$ matrix where each element is given by

$$A_{mn} = \begin{cases} 1 & \text{if there is a link from node } n \text{ to node } m \\ 0 & \text{otherwise} \end{cases} \tag{1.1}$$

This network is said to be unweighted or *binary* because the strength of all connections is the same. Notice that undirected networks are represented by symmetric adjacency matrices, $A = A^T$ where A^T denotes the transposed matrix.

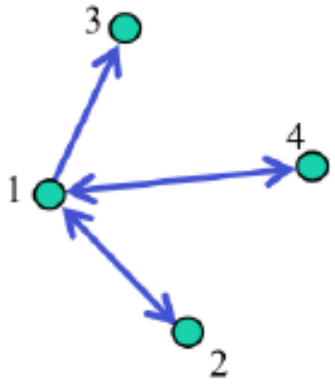

$$A = \begin{bmatrix} 0 & 1 & 1 & 1 \\ 1 & 0 & 0 & 0 \\ 0 & 0 & 0 & 0 \\ 1 & 0 & 0 & 0 \end{bmatrix}$$

Figure 1.1: An adjacency matrix is constructed from the given network. Note that the network is directed and so the adjacency matrix is not symmetric. Also note that the newtork is not strongly-connected because there is no path from $3 \to 1$. From [19]

We are often also interested in *weighted* networks where the strength of the connections can vary. The *adjacency matrix* of a *weighted* network will have elements

$$A_{mn} = \begin{cases} \neq 0 & \text{if there is a link from node } n \text{ to node } m, \\ 0 & \text{otherwise,} \end{cases} \tag{1.2}$$

where the value of element A_{mn} is the strength of the connection from node n to node m, and no connection

implies the strength is 0. A weighted network may have varying link weights. An *unweighted* network has all links from strength 1. Although Eq. (1.1) is the formal definition of adjacency matrix, for the remainder of this paper we will use Eq. (1.2) to define *adjacency matrix* and the matrix defined in Eq. (1.1) will be called the *unweighted adjacency matrix*.

The weights in an adjacency matrix can be positive or negative, but for the analysis in this thesis they will always be non-negative. For the purpose of this thesis we will only consider *strongly-connected* networks, and the adjacency matrices derived from these. A network is strongly-connected if, for any given pair of nodes a and b, there is a path $a \to b$ and a path $b \to a$. Any nodes that are not strongly-connected to the others should be removed until we only consider one strongly-connected component. We are interested in the spectral properties of a strongly-connected nonnegative network which leads us to a statement of the Perron-Frobenius Theorem. There are variations for positive and non-negative matrices. A statement of the theorem will be given without proof. A proof can be found in [20].

Perron-Frobenius Theorem: Let A be an irreducible non-negative $N \times N$ matrix with spectral radius λ. The following statements are true:

(1) There is a positive, real eigenvalue of A, denoted as λ, the Perron-Frobenius eigenvalue of A.

(2) The Perron-Frobenius eigenvalue λ is simple.

(3) Both the left and right eigenvectors associated with λ, denoted $\mathbf{u^T}$ and $\mathbf{v}$ respectively, have all positive entries.

(4) λ has the largest magnitude among all eigenvalues of A.

Note that if a graph is strongly-connected then its adjacency matrix is irreducible.

1.1.2 Degree Distributions

The adjacency matrix contains a complete and global description of the network, but we are often interested in the environment of individual nodes. One characterization of this local environment is the

number of incoming and outgoing links at each node. This leads us to define the degrees of the nodes

$$k_n^{in} = \sum_{m=1}^{N} A_{nm} \qquad \text{and} \qquad k_n^{out} = \sum_{m=1}^{N} A_{mn}. \tag{1.3}$$

The in-degree (out-degree) is the sum of all connections coming into (out of) a node. Note that this definition works equally well with weighted and binary networks. Lastly, we define the mean degree,

$$\langle k \rangle = \frac{1}{N} \sum_{n=1}^{N} k_n^{in} = \frac{1}{N} \sum_{n=1}^{N} k_n^{out} = \frac{1}{N} \sum_{n=1}^{N} \sum_{m=1}^{N} A_{mn}, \tag{1.4}$$

where $\langle \cdot \rangle$ denotes the average over nodes.

We are most interested in degree distributions that are observed for real-world networks. One observation that has helped develop modern network theory is that real-world degree distributions are often highly heterogeneous. A heterogeneous degree distribution means there is not a typical degree, but a potentially large range of degrees of the nodes. It has been found that degree distributions often follow a power-law, $P(k) = Ck^{-\gamma}$[21], and these will be the degree distributions studied in this paper. In particular, many real-world network degree distributions can be approximated by a power-law with an exponent between 2.1 and 3.5. Networks with a power-law degree distribution are often called *scale-free networks* because the ratio $P(ak)/P(k) = a^{-\gamma}$ does not depend on k, therefore the network cannot be characterized by any scale. One implication is that there will be *hubs*, highly connected nodes that play a crucial role in the dynamics of the network such as in epidemic spreading, neural excitations, and power grid performance.

Power-law degree distributions are often hard to study because it is not trivial to determine whether or not a given set of data really follows a power-law distribution [22]. The power-law scaling often does not hold for small k and the data will sometimes only span a few decades and have cut-off effects making it invalid for large values of k. Another property of power-law networks is that only a finite number of moments $E[k^m]$ do not diverge. In general, we can approximate the moments of a power-law with exponent γ as an integral where

$$E[k^m] \approx \int_{k_{min}}^{\infty} k^m P(k) dk = \frac{\gamma - 1}{\gamma - 1 - m} k_{min}^m, \tag{1.5}$$

for $\gamma > m + 1$ and diverges for $\gamma \leq m + 1$. Where we assume that the number of nodes tends to infinity, and the approximation becomes better as k_{min} grows. In a finite network the moments are finite, but will be very large if the corresponding moment for an infinite network would diverge.

Note that the in- and out-degrees do not have to be related. For example, If we view links as following someone on Twitter, a celebrity may have millions of followers (high in-degree), but only follow a handful of people (low out-degree). We wish to be able to estimate the probability that a randomly chosen node has a certain in-degree and out-degree. This leads us to define

$$P(k^{out}, k^{in}) = \text{probability that a randomly chosen node has out-degree } k^{out} \text{ and in-degree } k^{in}. \quad (1.6)$$

We can then define the marginal distributions for the in-degrees and out-degrees,

$$P_{out}(k^{out}) = \sum_{k^{in}} P(k^{out}, k^{in}) = \text{probability that a randomly chosen node has out-degree } k^{out}, \quad (1.7)$$

$$P_{in}(k^{in}) = \sum_{k^{out}} P(k^{out}, k^{in}) = \text{probability that a randomly chosen node has in-degree } k^{in}, \quad (1.8)$$

If the in-degree and out-degree are independent variables, then

$$P(k^{out}, k^{in}) = P_{in}(k^{in}) P_{out}(k^{out}). \quad (1.9)$$

1.1.3 Degree Correlations

In practice, in- and out-degree often depend on each other so it is helpful to quantify this interdependence. This leads us to define two types of degree correlations. The first, *node degree correlations* describe correlations between the in- and out-degree at the same node. Node degree correlations imply we can gain statistical information about a node's in-degree given its out-degree and vice versa. Rather than working with the more cumbersome distribution in Eq. (1.6), we are just looking to quantify the correlation between

in-degree and out-degree. Following Refs. [23, 24], we define the node correlation coefficient

$$\eta = \frac{\langle k^{in} k^{out} \rangle}{\langle k^{in} \rangle \langle k^{out} \rangle} = \frac{\langle k^{in} k^{out} \rangle}{\langle k \rangle^2}, \tag{1.10}$$

where $\langle \cdot \rangle$ denotes an average over nodes. A value $\eta > 1$ means the in- and out-degrees are positively correlated, $\eta < 1$ means they are negatively correlated, and $\eta = 1$ means they are independent. An alternative way to measure correlation is through the Pearson correlation coefficient [23]

$$r_{node} = \frac{\langle (k^{in} - \langle k \rangle)(k^{out} - \langle k \rangle) \rangle}{\sqrt{(\langle (k^{in} - \langle k \rangle)^2 \rangle)(\langle (k^{out} - \langle k \rangle)^2 \rangle)}}, \tag{1.11}$$

where $r < 0$ means negative correlations, $r = 0$ means no correlation, and $r > 0$ means positive correlations. Note that the Pearson correlation coefficient is simply a shift of the node correlation coefficient which centers the coefficient on 0, and normalizes it so that $-1 \leq r \leq 1$.

The second class of degree correlations, *edge degree correlations* are those which correlate the degrees of nodes at the end of a randomly chosen link. In particular, for a link connecting node n and node m, we will examine the correlations between k_n^{in}, k_n^{out}, k_m^{in}, and k_m^{out}. For a link from node n to node m we will focus on correlations between k_n^{in} and k_m^{out} since they will have the most influence on the dynamical processes. We define the correlation coefficient for edge degree correlations as [24]

$$\rho = \frac{\langle k_n^{in} k_m^{out} \rangle_e}{\langle k^{in} \rangle_e \langle k^{out} \rangle_e}, \tag{1.12}$$

where $\langle \cdot \rangle_e$ denotes the average over all edges in the network. A value $\rho < 1$ corresponds to negative correlations (Figure 1.2a), $\rho = 1$ corresponds to independence, and $\rho > 1$ corresponds to positive correlations (Figure 1.2b).

1.2 Model Used in This Thesis

We develop a theory of avalanche size and duration on complex networks that explicitly includes the network topology. This approach allows for an analysis of avalanches starting from arbitrary nodes in the

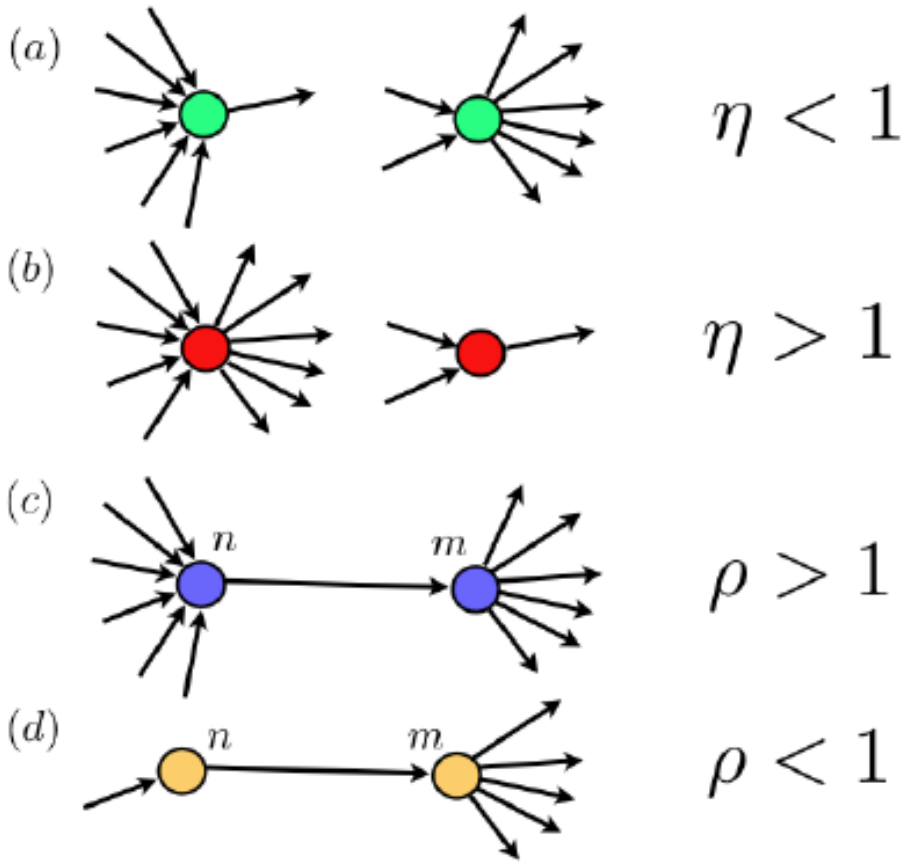

Figure 1.2: (a) the in-degrees and out-degrees are negatively correlated, (b) the in-degrees and out-degrees are positively correlated, (c) the degrees are positively correlated across the edge, (d) the degrees are negatively correlated across the edge. Figure from [19]

network and the effect of nontrivial network structure on the distribution of avalanches. In this paper we study the statistics of avalanches propagating in complex networks. While our formalism is very general, our analysis was motivated by recent experiments on avalanches of neuronal bursting in the mammalian cortex.

To model the propagation of avalanches on a network, we consider a network of N nodes labeled $m = 1, 2, ..., N$, each of which can be in one of two states, $\tilde{x}_m = 0$ or 1. We refer to the state $\tilde{x}_m = 0$ as the *resting* state and to $\tilde{x}_m = 1$ as the *excited* state. At discrete times $t = 0, 1, ...$, the states of the nodes $\tilde{x}_m^t$ are simultaneously updated as follows: (i) If node m is in the resting state, $\tilde{x}_m^t = 0$, it can be excited by an excited node n, $\tilde{x}_n^t = 1$, with probability $0 \leq A_{mn} < 1$, so that $\tilde{x}_m^{t+1} = 1$. (ii) The nodes that are excited, $\tilde{x}_n^t = 1$, will deterministically return to the ready state in the next time step, $\tilde{x}_n^{t+1} = 0$. We therefore describe a network of N nodes with a $N \times N$ weighted network adjacency matrix $A = \{A_{mn}\}$, where $A_{mn} \neq 0$ may be thought of as the strength of connection from node n to node m, and $A_{mn} = 0$ implies that node n does not connect to node m. We will assume that the network encoded by the weighted adjacency matrix A is strongly-connected (and therefore the adjacency matrix is irreducible).

Starting from a single excited node k ($\tilde{x}_j^0 = 1$ if $j = k$ and $\tilde{x}_j^0 = 0$ if $j \neq k$), we let the system evolve according to the dynamics above, and observe the cascade of activity until there are no more excited nodes. This motivates the following definitions, which are illustrated in Fig. 1.3 : (1) an *avalanche* is the sequence of excitations produced by a single excited node; (2) the *duration* d of an avalanche is defined as the total number of time steps spanned by the avalanche: if the avalanche starts with $\tilde{x}_k^0 = 1$, then

$$d_n = \min_{t \geq 0} \{\tilde{x}_k^t = 0 \text{ for all } k\}. \tag{1.13}$$

An avalanche that continues indefinitely is said to have infinite duration; (3) the *size* x of an avalanche starting at $\tilde{x}_n^0 = 1$ is defined as the total number of nodes excited during an avalanche, allowing for nodes to be excited multiple times:

$$x_n = \sum_{t=0}^{d-1} \sum_{k=1}^{N} \tilde{x}_k^t. \tag{1.14}$$

Note that it is possible for an avalanche to have size larger than the total size of the network. The main goal

of this thesis is to determine the probability distributions of these variables in terms of the matrix A.

Networks were constructed in two steps. First, binary networks (with adjacency matrix entries $\hat{A}_{mn} \in \{0, 1\}$) were constructed via an implementation of the configuration model [25], using $N = 10^5$ nodes, with nodal degrees drawn from a power-law distribution with exponent 3.5, i.e. the probability that a node has degree k is proportional to $k^{-3.5}$. Second, each nonzero entry $\hat{A}_{mn}$ was given a weight, drawn from a uniform distribution $\mathcal{U}[0, 1]$. We then calculated the Perron-Frobenius eigenvalue of this weighted matrix $\hat{A}$, $\lambda_{\hat{A}}$, and multiplied the matrix $\hat{A}$ by $\lambda/\lambda_{\hat{A}}$, resulting in a matrix A with the desired eigenvalue λ. We simulated avalanches for networks with λ between 0.5 and 1.5, sampling more finely for values close to 1.

Each simulated avalanche was created by first exciting a single network node, chosen uniformly at random, and then observing the size and duration of the resulting avalanche as defined in Eqs. (1.13) and (1.14). If the resulting avalanche lasted for more than 10^6 time steps, we considered it as having infinite duration and infinite size. In all cases, the initial excitation was included so that the minimum size was $x = 1$ and the minimum duration was $d = 1$. For each subcritical ($\lambda < 1$) and supercritical ($\lambda > 1$) cases, 10^6 avalanches were simulated, and for $\lambda = 1$, we simulated $2 \cdot 10^6$ avalanches to better sample the very broad distribution of avalanche sizes at criticality.

As will be discussed in detail in the following chapters, we find that the statistical properties of avalanches are determined by spectral properties of the matrix whose entries A_{mn} are the probabilities that the avalanche propagates from node n to node m. In particular, the Perron-Frobenius eigenvalue λ and its associated eigenvectors play a prominent role in determining the functional form and the parameters for the statistical distribution of avalanche sizes and durations. While many of our findings have analogous results in classical Galton-Watson branching processes [2, 3], we emphasize that our analysis allows us to identify how changes in network structure affect the parameters of the statistical distributions of avalanche sizes and durations. Moreover, our theory allows us to find the statistical distributions of avalanches starting at particular network nodes.

This thesis is broken down into several chapters. Chapter 2 will derive and discuss the statistics for avalanche duration on excitable networks, classifying networks above, below, and at criticality, then numerically verifying our predictions with simulated experiments. Chapter 3 uses results from chapter 2

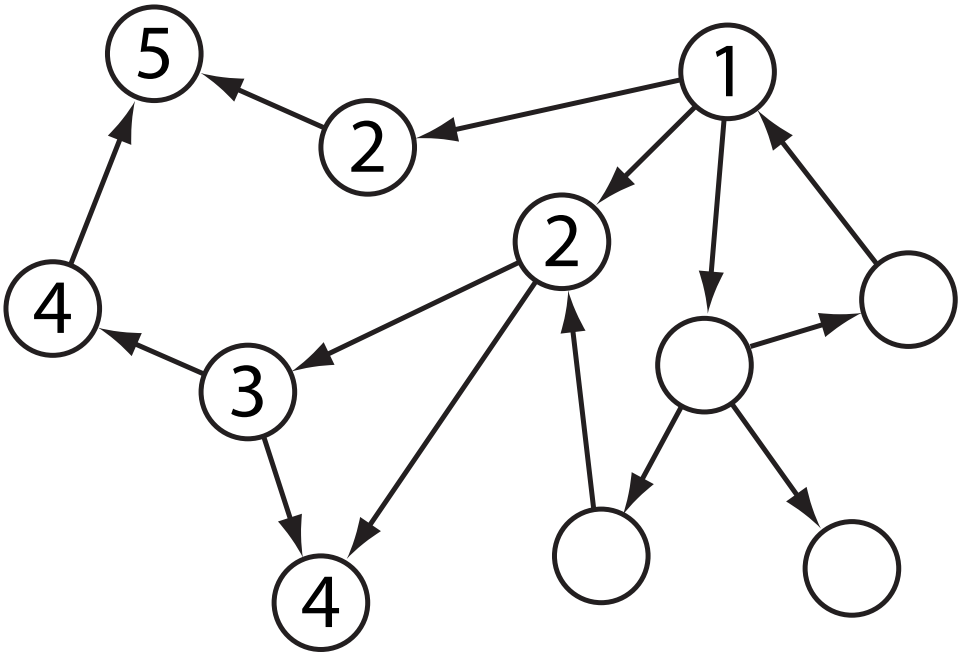

Figure 1.3: An example avalanche is shown, where circles represent nodes, arrows represent links, and numbers inside nodes correspond to the time step at which each node is activated. Starting from a single excited node, labeled 1, the avalanche spreads to two other nodes, labeled 2, and so on. Note that the presence of a link does not guarantee the transmission of excitation. The example avalanche above lasts for five time steps and excited a total of six nodes in addition to the initial node, so $d = 5$ and $x = 7$.

but the arguments are modified to find the distribution of sizes, also numerically verified with simulated experiments, and validated with data from slices of rat cortex and awake monkeys. Chapter 4 contains a discussion of results and implications of our research.

Chapter 2

Distribution of Avalanche Duration

The purpose of this chapter is to determine how the duration of an avalanche depends on the properties of the network. In particular, it is determined that networks can be separated into three distinct categories depending on the largest eigenvalue (λ, the Perron-Frohbenius eigenvalue) of the adjacency matrix. Networks with $\lambda = 1$ will be referred to as critical networks, $\lambda > 1$ as supercritical, and $\lambda < 1$ as subcritical. The goal of this chapter is to determine the distribution of avalanche duration for each of these classifications.

In order to analyze the statistics of avalanche durations, we define $c_n(t)$ as the probability that an avalanche starting at node n has duration less than or equal to t,

$$c_n(t) = \mathrm{P}(d_n \leq t). \tag{2.1}$$

The quantity $c_n(t)$ is the cumulative distribution function (CDF) of the random variable d_n. Here, we will restrict our attention to the class of *locally tree-like* networks [26], which can be approximated locally as simple directed trees. Many networks found in applications are of this type, and it is found that the locally tree-like approximation works very well in describing various dynamical process while still capturing the effects of network heterogeneity [13, 14, 27, 26, 28]. For these networks we can approximately treat the avalanches propagating to different neighbors of node n as independent when the total number of nodes is large. Exploiting this assumed independence, we can write the recursion relation,

$$c_n(t+1) = \prod_{m=1}^{N} \Big[(1 - A_{mn}) + A_{mn} c_m(t) \Big], \tag{2.2}$$

together with $c_n(0) = 0$ which follows from the definition (2.1). The right hand side of Eq. (2.2) is the probability that the nodes excited by node n generate themselves avalanches of duration at most t. The term $(1 - A_{mn})$ inside the product is the probability that an excitation *does not* pass from node n to node m, whereas $A_{mn}c_m(t)$ is the probability that an excitation *does* pass from node n to node m and the resulting avalanche has duration at most t. Note that Eq. (2.2) can treat any node n as the starting node for an avalanche. As discussed above, Eq. (2.2) assumes that the descendent branches of the avalanche are independent. In a complex network, where cycles of many lengths exist, it is possible that an avalanche may branch in such a way that two branches interact at a later time. However, for the networks we studied we found that, while these effects do occur for large avalanches, they do not significantly affect our predictions. These effects are minimized in larger networks since the probability of interacting is reduced.

Here we establish that the probability of finite avalanches, under our assumptions, is always 1 when $\lambda \leq 1$ (critical and subcritical networks), and becomes less than 1 when $\lambda > 1$ (supercritical networks). To do this we define $b_n = \lim_{t\to\infty} c_n(t)$ as the fixed point of the system described by Eq. (2.2) and therefore satisfies the equation

$$b_n = \prod_{m=1}^{N} \Big[(1 - A_{mn}) + A_{mn}b_m\Big]. \tag{2.3}$$

We are interested in the distribution of long avalanche durations, i.e., in the asymptotic form of $c_n(t)$ for $t \to \infty$. By definition, $c_n(t)$ is a bounded, increasing function of t and therefore it must converge to a value $\lim_{t\to\infty} c_n(t) = b_n \leq 1$ which can be interpreted as the probability that an avalanche starting at node n has finite duration. Our analysis will be based on the value of the fixed point, whether or not this limit is less than or equal to one, and determining the approach pattern to the fixed point. As shown in the remaining parts of this chapter, this is determined by the Perron-Frobenius eigenvalue of A, λ. If $\lambda < 1$ (subcritical), then $\lim_{t\to\infty} c_n(t) = 1$ with an exponential approach. In the case $\lambda = 1$ (critical), $\lim_{t\to\infty} c_n(t) = 1$ with a power-law approach. On the opposite side of the bifurcation, if $\lambda > 1$ (supercritical), then $\lim_{t\to\infty} c_n(t) = b_n < 1$ with an exponential approach. $b_n < 1$ implies that there is a non-zero probability that an avalanche has infinite duration. The asymptotic form of $c_n(t)$ will be analyzed separately for these three cases below.

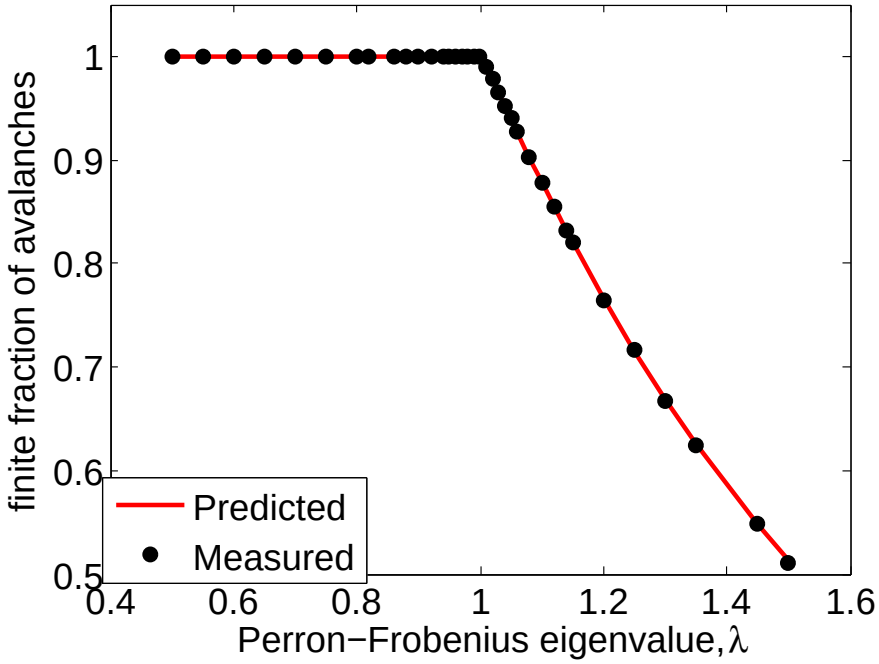

Figure 2.1: When the Perron-Frobenius eigenvalue λ is larger than one, there is a non-zero probability of an avalanche starting at node n having infinite duration, as predicted by Eq. (2.3). Here we average the finite fraction of avalanches originating from node n over all nodes, showing excellent agreement between the fraction predicted by averaging Eq. (2.3) (red line) and fraction measured from simulation (circles).

2.1 Subcritical Networks ($\lambda < 1$)

First, we show that if $\lambda < 1$, then the only solution to the equation above is $b_n = 1$. Letting $b_n = 1 - f_n$, we have for all n

$$1 - f_n = \prod_{m=1}^{N} \Big[1 - A_{mn} f_m\Big]. \tag{2.4}$$

Applying the Weierstrass product inequality to Eq. (2.4), we obtain

$$\sum_{m=1}^{N} A_{mn} f_m \geq f_n, \tag{2.5}$$

with equality only if $A_{mn} f_m = 0$ for all m. If $\mathbf{u}$ is the right Perron-Frobenius eigenvector of A, then left-multiplying Eq. (2.5) by $\mathbf{u}^T$ results in

$$\mathbf{u}^T A^T \mathbf{f} = \lambda \mathbf{u}^T \mathbf{f} \geq \mathbf{u}^T \mathbf{f}. \tag{2.6}$$

If there is a nonzero f_n, then $\mathbf{u}^T \mathbf{f} > 0$ since the Perron-Frobenius eigenvector has positive entries. Therefore, if $\lambda < 1$ we must have $f_n = 0$ for all n.

From the argument above, we find that in the subcritical case, $b_n = 1$ is the only fixed point of the system Eq. (2.2). To analyze the asymptotic form of $c_n(t)$, we assume it is close to the fixed point and define the small quantity

$$f_n(t) = b_n - c_n(t) = 1 - c_n(t). \tag{2.7}$$

Inserting this into Eq. (2.2) and linearizing we obtain

$$\begin{aligned} 1 - f_n(t+1) &= \prod_{m=1}^{N} \left[1 - A_{mn} f_m(t)\right] \\ f_n(t+1) &= \sum_{m=1}^{N} A_{mn} f_m(t). \end{aligned} \tag{2.8}$$

Assuming exponential decay (or growth) of perturbations, $f_n(t) = \lambda^t v_n$, we obtain

$$\lambda v_n = \sum_{m=1}^{N} A_{mn} v_m. \tag{2.9}$$

Thus, λ is an eigenvalue of A and $\mathbf{v}$ its left eigenvector. We identify λ as the Perron-Frobenius eigenvalue since, having the largest magnitude among all the eigenvalues, $\lambda^t v_n$ will be the dominant term as $t \to \infty$ when compared with the other modes. We note that for finite t, this approximation is good as long as there is a large enough separation between λ and the rest of the spectrum of A. This issue is discussed in [29], where it is found that this separation is typically large in networks without strong community structure. Henceforth, we will assume that λ is well separated from the rest of the spectrum of A.

Therefore, $c_n(t)$ approaches 1 exponentially since

$$c_n(t) \approx 1 - \lambda^t v_n, \tag{2.10}$$

where $\mathbf{v}$ is the left eigenvector of A corresponding to λ, which has positive entries by the Perron-Frobenius theorem [20]. We note that from the standpoint of nonlinear dynamics, the fixed point $b_n = 1$ is linearly stable when $\lambda < 1$.

The probability density function (PDF) of avalanche durations is given by $p_n(t) = P(d_n = t) = c_n(t) - c_n(t-1)$, so

$$p_n(t) = (\lambda^{-1} - 1)\lambda^t v_n, \tag{2.11}$$

which decays exponentially to zero with decay rate $|\ln(\lambda)|$.

In summary, we can draw two predictions from the analysis above for subcritical networks: (i) the PDF of avalanche duration will decay exponentially towards zero as λ^t, and (ii) the probability that an avalanche started at node n lasts more than t steps is proportional to the n^{th} entry of the left eigenvector of A, v_n. These predictions are tested in Sec. 2.4.

2.2 Supercritical networks ($\lambda > 1$)

Now, we show that if $\lambda > 1$ then $\lim_{t\to\infty} c_n(t) = b_n < 1$. To show this, we view Eq. (2.2) as a dynamical system and note that the analysis of Sec. 2.1, applied to the case $\lambda > 1$, shows that the fixed point $b_n = 1$ is linearly unstable. If we show that $c_n(t)$ are nondecreasing with t, then their limit b_n must be less than one. We will prove by induction that $c_n(t+1) \geq c_n(t)$ for all n. First, we have $c_n(0) = 0$ and $c_n(1) = \prod_m (1 - A_{nm}) \geq 0$, so the statement is valid for $t = 0$. Then, assume $c_m(t) \geq c_m(t-1)$ for all m and consider $c_n(t+1)/c_n(t)$ (assuming $c_n(t) > 0$):

$$\begin{aligned}\frac{c_n(t+1)}{c_n(t)} &= \prod_{m=1}^{N} \frac{(1 - A_{mn}) + A_{mn}c_m(t)}{(1 - A_{mn}) + A_{mn}c_m(t-1)} \\ &= \prod_{m=1}^{N} \left[1 + \frac{A_{mn}(c_m(t) - c_m(t-1))}{(1 - A_{mn}) + A_{mn}c_m(t-1)}\right] \\ &\geq 1, \end{aligned} \tag{2.12}$$

which proves the desired statement. Although from the definition (2.1), $c_n(t)$ are nondecreasing, note that this proof is necessary since Eq. (2.2) is an approximation to the CDF.

We have shown that there exists another fixed point b_n to which $c_n(t)$ converges from below: $\lim_{t\to\infty} c_n(t) = b_n < 1$. Thus, there is a non-zero probability that an avalanche will have infinite duration. Our analysis below characterizes the distributions of finite avalanche durations in supercritical networks. Recall from Eq. (2.3) that the fixed point b_n satisfies

$$b_n = \prod_{m=1}^{N} \Big[(1 - A_{mn}) + A_{mn}b_m\Big]. \tag{2.13}$$

Again, we introduce the quantity $f_n(t) = b_n - c_n(t)$, and consider the limit when t is large and f_n is small. We substitute this into Eq. (2.2) and rewrite it as

$$b_n - f_n(t+1) = b_n \prod_{m=1}^{N} \Big[1 - \frac{A_{mn}f_m(t)}{(1 - A_{mn}) + A_{mn}b_m}\Big]. \tag{2.14}$$

By defining a new matrix D with entries

$$D_{mn} = \frac{A_{mn} b_n}{(1 - A_{mn}) + A_{mn} b_m}, \tag{2.15}$$

and linearizing Eq. (2.14), we find:

$$f_n(t+1) \approx \sum_{m=1}^{N} D_{mn} f_m(t). \tag{2.16}$$

As in the subcritical case, we conclude that $f_n(t) \approx \lambda_D^t w_n$, where $\mathbf{w}$ is the left Perron-Frobenius eigenvector of the matrix D and λ_D its Perron-Frobenius eigenvalue. Therefore, we have

$$c_n(t) \approx b_n - w_n \lambda_D^t. \tag{2.17}$$

To ensure that this fixed point is stable, we can show that $\lambda_D \leq 1$ and equality holds only when $\lambda = \lambda_D = 1$. To prove this short lemma we will consider Eq. (2.13) and parametrize it according to a variable α.

$$b_n(\alpha) = \prod_{m=1}^{N} [1 - \alpha A_{mn} + \alpha A_{mn} b_m], \tag{2.18}$$

where α is a scaling parameter on A which uniformly strengthens or weakens all connections in the network. We will consider the derivative of the b_n's with respect to α. Through a repeated product rule, the derivative of the product transforms into a sum.

$$\frac{db_n}{d\alpha} = b_n(\alpha) \sum_{m=1}^{N} \frac{-A_{mn} + A_{mn} b_m + \alpha A_{mn} \frac{db_m}{d\alpha}}{1 - \alpha A_{mn} + \alpha A_{mn} b_m}. \tag{2.19}$$

Next we will evaluate this entire expression at $\alpha = 1$ to recover the original b_n, and we will denote $\frac{db_n}{d\alpha}(\alpha = 1)$ as z_n;

$$z_n = \sum_{m=1}^{N} \Big[\frac{A_{mn} b_n}{1 - A_{mn} + A_{mn} b_m} (-1 + b_m + z_m) \Big] \tag{2.20}$$

$$= \sum_{m=1}^{N} D_{mn} (-1 + b_m + z_m). \tag{2.21}$$

.

We can express this as a vector equation and, rearranging, we find

$$D^T \mathbf{z} - \mathbf{z} = D^T (\mathbf{1} - \mathbf{b}). \tag{2.22}$$

Left multiplying by $\mathbf{w}^T$ the Perron-Frobenius eigenvector of D, Eq. (2.22) simplifies to

$$(\lambda_D - 1) w^T \mathbf{z} = \lambda_D w^T (\mathbf{1} - \mathbf{b}) \tag{2.23}$$

From the definition, we can see that D has all non-negative entries, and therefore a positive Perron-Frobenius eigenvalue. From the definition of the b_n and the stability analysis of the $b_n = 1$, we can see that each $b_n < 1$ so the vector $(\mathbf{1} - \mathbf{b})$ has all non-negative entries. Additionally every element of w^T is positive by the Perron-Frobenius theorem, and $\lambda_D > 0$ so the right hand side has all positive entries. We know that every element of $\mathbf{z}$ is non-positive because increasing the connectivity of the network can't possibly decrease the probability of a finite avalanche. This claim is verified numerically in Fig. 2.3 which plots average b_n vs. λ (if A is a fixed network with largest eigenvalue of 1 then α and λ are identical). From these arguments we see that $\lambda_D w^T (\mathbf{1} - \mathbf{b}) > 0$, and $w^T \mathbf{z} < 0$ is negative, therefore $\lambda_D < 1$.

These results lead to two predictions: (i) the PDF of avalanche duration will decay exponentially towards zero as λ_D^T in supercritical networks, and (ii) the probability that an avalanche started at node n lasts more than t steps is proportional to the n^{th} entry of the left eigenvector of D, w_n. These predictions are tested and discussed in Sec. 2.4. We note that these predictions simplify to those drawn from Eq. (2.10) if the network is subcritical. In this case $b_n = 1$, Eq. (2.15) simplifies to $D_{mn} = A_{mn}$, and therefore $\lambda_D = \lambda$

and $\mathbf{v} = \mathbf{w}$.

2.3 Critical Networks ($\lambda = 1$)

If $\lambda = 1$, we return to the Weierstrass inequality and its result in Eq. (2.6).

$$\mathbf{u}^T A^T \mathbf{f} = \lambda \mathbf{u}^T \mathbf{f} \geq \mathbf{u}^T \mathbf{f}. \tag{2.24}$$

The case $\lambda = 1$ implies equality in Eq. (2.5), which implies either (i) $A_{mn} f_m = 0$ for all m, and thus $f_n = 0$ by (2.5), or (ii) $A_{mn} f_m = 0$ for all $m \neq k$ and $A_{kn} f_k = 1$ for some k, which is impossible since we assumed that the entries of A are strictly less than one and f_k is a probability. Therefore, we must have $f_n = 0$ if $\lambda = 1$, and this argument is valid for any n. Together with the previous argument above, we conclude that $b_n = 1$ for all n if $\lambda \leq 1$.

The analyses in Sec. 2.1 and 2.2 show that if $\lambda = 1$, the fixed point $b_n = 1$ is marginally stable. The linear stability analysis yields neither stability nor instability and higher order terms need to be considered. This fixed point must be an attracting fixed point, since $c_n(t)$ is nondecreasing and $b_n = 1$ is the only fixed point of Eq. (2.2). To determine the asymptotic form of $c_n(t)$ for large t, we let $c_n(t) = 1 - f_n(t)$. We assume that Eq. (2.2) has a solution whose asymptotic functional form in t (to be determined) can be extended to a differentiabe function of a continuous time variable t. Since the convergence of $f_n(t)$ to 0 is slower than exponential in the critical case, we look for a solution $f_n(t)$ which is slowly varying in t when $f_n(t)$ is small, and approximate

$$f_n(t+1) \approx f_n(t) + f_n'(t). \tag{2.25}$$

The slowly varying assumption implies that $f_n'(t) \ll f_n(t)$ as $f_n \to 0$, which we note excludes an exponential solution. Substituting Eq. (2.25) into Eq. (2.2), we get

$$1 - f_n(t) - f_n'(t) \approx \prod_{m=1}^{N} \left[1 - A_{mn} f_m(t)\right]. \tag{2.26}$$

Assuming $f_n(t) \ll 1$ and expanding to second order, we get after simplifying and dropping the time notation

for clarity,

$$f_n + f_n' \approx \sum_m A_{mn} f_m - \frac{1}{2} \sum_m \sum_{k \neq m} A_{mn} A_{kn} f_m f_k. \tag{2.27}$$

The leading order terms are f_n on the left-hand side and $\sum_m A_{mn} f_m$ on the right-hand side, so for these to balance as $f \to 0$ requires

$$f_n = \sum_m A_{mn} f_m. \tag{2.28}$$

Therefore, in this limit the vector $\mathbf{f}(t) = [f_1(t), f_2(t), \ldots, f_N(t)]^T$ has to be proportional to the normalized left eigenvector $\mathbf{v}$ of A with eigenvalue $\lambda = 1$. Thus, a slowly varying solution only exists for a critical network. Since $\mathbf{v}$ is independent of time, the constant of proportionality must be time dependent, $f_n(t) = K(t) v_n$. Now, for finite f, we expect the solution to deviate by a small error from this limit solution, so we set

$$f_n(t) = K(t) v_n / \langle v \rangle + \varepsilon_n(t), \tag{2.29}$$

where we assume $\varepsilon_n \ll f_n(t)$, $\varepsilon_n' \ll f_n'(t)$, and the term $\langle v \rangle = \sum_{n=1}^N v_n / N$ is included to make $K(t)$ independent of the normalization of $\mathbf{v}$. Inserting this in Eq. (2.27), neglecting terms of order ε', ε^2, $f\varepsilon$, and using $\sum_m \sum_{k \neq m} A_{mn} A_{kn} v_m v_k \approx v_n^2$, we obtain

$$\varepsilon_n + K'(t) v_n / \langle v \rangle = \sum_{m=1}^N A_{mn} \varepsilon_m - \frac{1}{2} K^2(t) v_n^2 / \langle v \rangle^2 \tag{2.30}$$

To eliminate the unknown error term ε, we multiply by u_n, where $\mathbf{u}$ is the right eigenvector of A satisfying $\mathbf{u}^T A^T = \mathbf{u}^T$, and sum over n. The error terms cancel and we obtain an ordinary differential equation (ODE),

$$K'(t) = -\frac{1}{2} \frac{\langle uv^2 \rangle}{\langle uv \rangle \langle v \rangle} K^2(t), \tag{2.31}$$

where $\langle xy \rangle \equiv \frac{1}{N} \sum_n x_n y_n$. Solving this ODE yields

$$K(t) \approx \frac{1}{\beta + \frac{1}{2} \frac{\langle uv^2 \rangle}{\langle uv \rangle \langle v \rangle} t}, \tag{2.32}$$

where β is an integration constant. In terms of the original variables, we obtain

$$c_n(t) \approx 1 - \frac{v_n}{\beta + \frac{1}{2} \frac{\langle uv^2 \rangle}{\langle uv \rangle \langle v \rangle} t}. \tag{2.33}$$

The PDF, in the continuous time approximation, is given by $p_n(t) = -c_n'(t)$,

$$p_n(t) \propto \frac{v_n}{\left(\beta + \frac{1}{2} \frac{\langle uv^2 \rangle}{\langle uv \rangle \langle v \rangle} t\right)^2} \tag{2.34}$$

From Eq. (2.34) we make the prediction that as $t \to \infty$, $1 - c_n(t) \sim t^{-1}$. This prediction is tested in Sec 2.4.

As a brief summary of the predictions for avalanche duration distributions, we predict that the probability of an avalanche of duration d will decay as λ^d for subcritical networks ($\lambda < 1$), as d^{-2} for critical networks ($\lambda = 1$), and as λ_D^d for supercritical networks ($\lambda > 1$), where λ_D is the Perron-Frobenius eigenvalue of matrix given in Eq. (3.7).

2.4 Numerical Verification

This section serves to provide numerical verification for the theory developed in this chapter. We construct networks by using the configuration model as described below, and then rescaling the adjacency matrix to rescale the spectrum. We simulate avalanches moving over these networks where the weight for each connection represents the probability an excitation will pass from one node to another as described in Sec. 1.2. By performing these simulations, we are able to measure all statistics for avalanches and verify our predictions.

The first task to conquer is to be able construct networks (encoded in an adjacency matrix A) with the

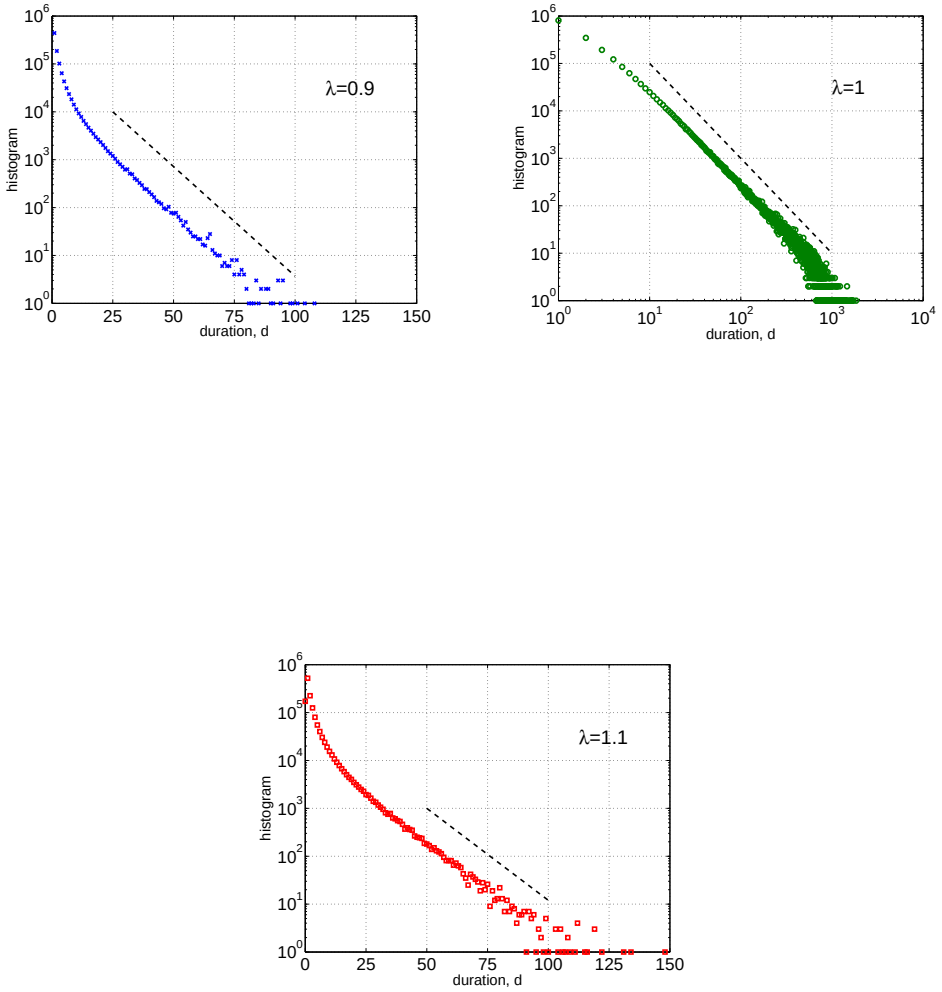

Figure 2.2: Histograms of avalanche durations shown above for networks of $N = 10^5$ nodes with power law degree distribution, exponent $\gamma = 3.5$ with Perron-Frobenius eigenvalues of $\lambda = 0.9$ (top left), $\lambda = 1.0$ (top right) and $\lambda = 1.1$ (bottom). Data are the exact recorded histograms from a single simulation of 10^6, $2 \cdot 10^6$, and 10^6 avalanches respectively from left to right. Dashed lines provide a reference for the theoretical predictions described in Eqs. (2.10), (2.33), and (2.17). Due to predictions of exponential decay for the sub- and super-critical cases, the left and right plots are log-linear scale, while the center plot is log-log to show the power-law decay. Infinite duration avalanches in the supercritical case (bottom) are not represented in the data set.

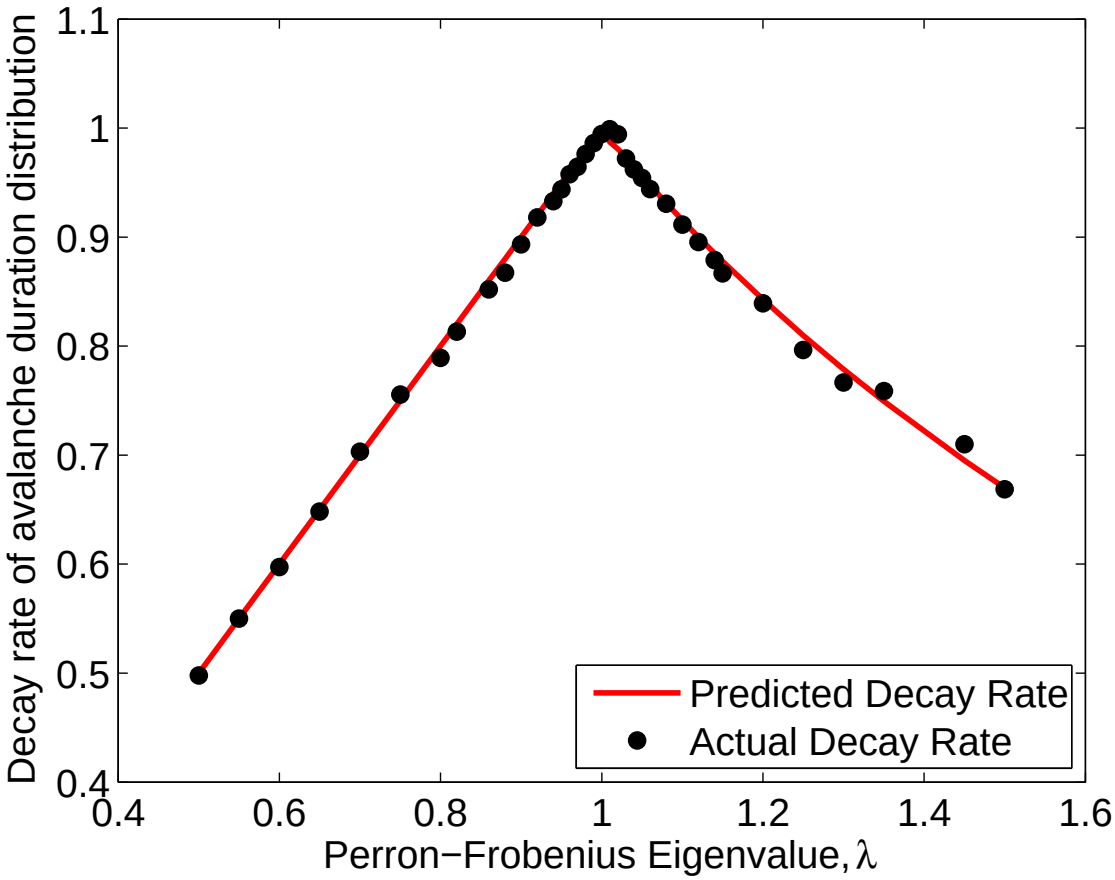

Figure 2.3: A comparison of predicted duration decay rates [Eq. (2.10) and Eq. (2.17)] (red line), and numerical simulations (circles) plotted against λ, the largest eigenvalue of the network adjacency matrix. Agreement is excellent for both the subcritical and supercritical numerical simulations.

desired properties so that we can simulate avalanches. The *configuration model* [25] was used to construct the networks in this paper. The goal is that given a target degree sequence $k = [k_1, k_2, ..., k_N]$, we wish to uniformly choose a simple network with degree sequence k from the ensemble of all simple networks with degree sequence k. In practice, there are several hurdles to overcome. Consider the degree sequence $k = [5, 5, 1, 1, 1, 1]$. It is impossible to construct a simple network with the given degree sequence. Another possible problem arises if the total number of links is odd since each link connects two nodes it must be even, or in the case of directed networks, if $\sum k^{in} \neq \sum k^{out}$. A *graphic sequence* is a sequence of numbers such that there exists some simple graph with that particular degree sequence. Conditions for graphic sequences can be found in Ref. [30].

If the given degree sequence can possibly be constructed, then we construct graphs from the degree sequence with uniform probability. To do this we set up N nodes and at each node n we place k_n "stubs" or half-links. We randomly choose pairs of stubs to connect until all stubs form into links. If the resulting network is simple (i.e., there are no self-connections or double edges) then the network is accepted. If not then the network is rejected and the process is attempted again until a satisfactory network is created. This model is called the "repeated configuration model" [31].

Since it may be necessary to repeat this process many times, we will estimate the probability that this construction will actually succeed. Define the probability p_{ij} that node i is connected to node j. Each of the k_i stubs at node i can connect to any of the other $2m - 1$ stubs with equal probability, so the probability that each stub at node i connects to node j is $\frac{k_j}{2m-1}$. Therefore the probability that there is at least one connection from node i to node j can be approximated by

$$p_{ij} \approx \frac{k_i k_j}{2m-1} \approx \frac{k_i k_j}{N\langle k \rangle}. \tag{2.35}$$

Notice we run into a problem if $\frac{k_i k_j}{2m-1} = O(1)$. Similarly, a more precise argument shows

$$\begin{aligned} p_{ij} &= 1 - P(\text{there is no connection}) \\ &= 1 - \left(\frac{2m-1-k_j}{2m-1}\right)^{k_i} \\ &= 1 - \left(1 - \frac{k_j}{2m-1}\right)^{k_i} \\ &\approx \frac{k_i k_j}{2m-1} \approx \frac{k_i k_j}{N\langle k\rangle} \end{aligned} \tag{2.36}$$

as long as $\frac{k_i k_j}{2m-1} \ll 1$, which agrees with our previous argument.

Next we find the probability that there are at least two connections between nodes i and j. P(at least two connections) = P(at least two connections $\mid$ at least one connection) P(at least one connection).

$$P(2 \text{ connections}) \approx \frac{(k_i-1)(k_j-1)}{2m} \frac{k_i k_j}{2m}, \tag{2.37}$$

which we sum over all pairs of nodes (i, j) and dividing by 2 to avoid double counting (i, j) and (j, i).

$$\begin{aligned} E[\#\text{ nodes with multiple edges}] &= \frac{1}{2} \sum_{i,j} \frac{k_i(k_i-1)k_j(k_j-1)}{N^2\langle k\rangle^2} \\ &= \frac{1}{2} \left(\frac{\langle k^2\rangle - \langle k\rangle}{\langle k\rangle^2}\right)^2. \end{aligned} \tag{2.38}$$

Next we divide by N to find the fraction of nodes with multiple edges,

$$f = \frac{1}{2N} \left(\frac{\langle k^2\rangle - \langle k\rangle}{\langle k\rangle^2}\right)^2, \tag{2.39}$$

so if $\langle k^2\rangle$ is finite, then $f \sim \frac{1}{N} \to 0$ as $N \to \infty$. From Eq. (1.5) we know that $\langle k^2\rangle$ diverges for exponents $\gamma \leq 3$ and converges for $\gamma > 3$, so for power-law networks with exponent $\gamma > 3$ then the fraction of nodes with double links goes to 0 as $N \to \infty$. Actually, we can go one step further by evaluating Eq. (1.5) and

taking the limit we see that $\langle k^2 \rangle \sim N^{3-\gamma}$. Assuming that $\langle k \rangle$ is finite then

$$f \sim \frac{1}{N}(N^{3-\gamma})^2 = N^{5-2\gamma} \begin{cases} \to 0 & \text{if } \gamma > 2.5 \\ \to \infty & \text{if } \gamma < 2.5 \end{cases} \tag{2.40}$$

So for power-law degree distributions with exponent $\gamma > 2.5$ then the fraction of nodes with multiple edges goes to zero as $N \to \infty$ and the configuration model is a viable method for constructing the network.

Once we have generated a complex network as described above, a large number (usually 10^6) of avalanches are simulated on these networks so that we can construct a histogram for avalanche duration which will serve as an approximation to the PDF. From the PDF we can approximate the rate at which the PDF decays towards its fixed point. In Fig. 2.2, the PDF is plotted against our predicted decay rates. The scales on the plots are designed so that the PDF will decay as a straight line. The plots are logarithmic on the y-axis for subcritical and supercritical networks and both the x and y-axes are logarithmic for critical networks.

To numerically test the agreement between theory and experiment for the distribution of avalanche durations across the whole spectrum of λ, in Fig. 2.3 we compare the multiplicative decay rates (i.e. λ) predicted in Eqs. (2.10) and (2.17) (solid red line) with decay rates measured from data, calculated through a least-squares regression on the simulated PDF of avalanche duration to fit the data to an exponential decay of the form λ^t. The agreement is excellent over the entire range of λ values simulated.

Beyond aggregate statistics, we also test a more subtle prediction of Eq. (2.10). In Sec. 2.1, we concluded that $f_n(t) = 1 - c_n(t)$, where $f_n(t)$ represents the probability that an avalanche started at node n lasts more than t steps. For large t, $f_n(t) \propto \lambda^t v_n$, where $\mathbf{v}$ is the left Perron-Frobenius eigenvector of A. Other research in the network adjacency matrix literature has noted that the vector of nodal out-degrees (in-degrees) is a good approximation for the right (left) dominant eigenvector of A in the absence of degree correlations [24]. In this light, our prediction above is understandable: when there are not degree correlations in the network, then the out-degree of a node is a good first-order approximation to the eigenvector entry. A node with a larger right eigenvector entry (and thus larger out-degree) will tend to produce longer avalanches.

In order to fully test our prediction, we created networks with *assortative (disassortative) mixing by degree* [32], and measured this degree correlation using the coefficient defined in Eq. (1.12) [24],

$$\rho = \frac{\langle k_n^{in} k_m^{out} \rangle_e}{\langle k_n^{in} \rangle_e \langle k_m^{out} \rangle_e}, \tag{2.41}$$

where $\langle \cdot \rangle_e$ denotes an average over all edges and k are weighted nodal degrees defined as $k_n^{in} = \sum_m A_{mn}$ and $k_n^{out} = \sum_m A_{nm}$.

We created Erdős-Rényi random networks (as described in Ref. [33]) with $N = 10^4$ nodes, and rewired the network via a link-swapping process (as described in Ref. [24]) until we had very assortative and disassortative networks ($\rho = 1.2$ and $\rho = 0.8$, respectively). In these networks the out-degree is *not* a good approximation to the corresponding eigenvector entry. Eq. (2.10) implies that in such networks, the tails of the CDF of avalanches originating at node n will be proportional to the corresponding entry of the right eigenvector, but not necessarily to the nodal out-degree. In Fig. 2.4, we plot $f_n(30)$ and its corresponding entry in the right dominant eigenvector v_n for each node for a subcritical network with eigenvalue $\lambda = 0.95$ and with assortativity $\rho = 0.8$, showing that proportionality is excellent. In the inset of the same figure we plot $f_n(30)$ and against corresponding out-degree k_n^{out} for each node n, showing that proportionality to out-degree is poor for disassortative networks. Highly assortative networks produce the same effect, but are not shown here.

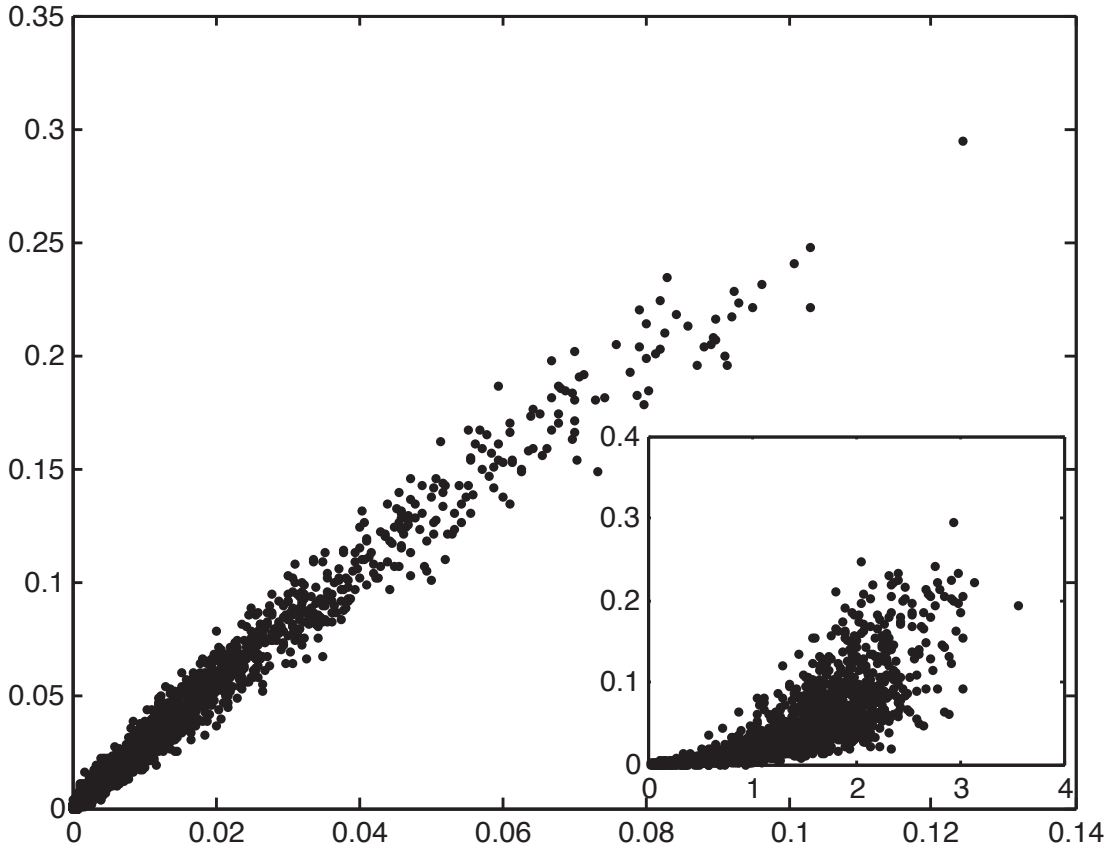

Figure 2.4: Testing the node-specific prediction of Eq. (2.10), avalanches were simulated on a subcritical ($\lambda = 0.95$) and disassortative ($\rho = 0.8$) Erdős Rényi random network with $N = 10^4$ nodes. In the large plot, the fraction of avalanches originating at node n that last longer than 30 time steps, $f_n(30)$ is plotted against the corresponding entry in the right Perron-Frobenius eigenvector, v_n. In the inset, the same values $f_n(30)$ are plotted against the corresponding out-degree k_n^{out}. The eigenvector entry v_n does a significantly better job than out-degree k_n^{out} of predicting the duration of avalanches originating at node n in disassortative networks (shown) and for assortative networks (not shown).

Chapter 3

Distribution of Avalanche Sizes

Similar to avalanche duration, we are interested in determining the statistics for the size of avalanches. In the experiments that motivated this work [11, 16, 18, 10], the size represents the aggregate neural activity during a single cascade and may be more easily measured via electrode implants. In these studies, avalanche sizes are measured based on the number of electrodes that are stimulated or on the total voltage received by all electrodes, both of which are directly analagous to avalanche size.

In order to analyze the distribution of avalanche sizes, we define the random variable x_n as the size of an avalanche starting at node n. Let z_{mn} be a random variable which is 1 if node n excites node m and 0 otherwise, so that $z_{mn} = 1$ with probability A_{mn} and 0 with probability $1 - A_{mn}$. Thus

$$x_n = 1 + \sum_m z_{mn} x_m. \tag{3.1}$$

From Sec. 2.2, we know that there is a non-zero probability that an avalanche has infinite duration, and therefore infinite size, when $\lambda > 1$. Therefore, we restrict our attention only to the distribution of avalanches that are finite. To study this distribution, we define the moment generating function

$$\phi_n(s) \equiv E[e^{-sx_n} | x_n < \infty]. \tag{3.2}$$

We now use Eq. (3.1) to derive a relation between the moment generating functions of different nodes. First, we rewrite the condition $x_n < \infty$ for node n in terms of events applicable to its neighbors. An avalanche starting at node n is finite if and only if for every node m, either (i) the excitation does not pass

from node n to node m, or (ii) the excitation passes from node n to node m but the subsequent avalanche starting from node m is finite. Therefore, we rewrite the condition $x_n < \infty$ as the requirement that for any m, $(z_{mn}, x_m) \in Z_{mn} \cup W_{mn}$, where we have defined the disjoint sets of events $Z_{mn} = \{z_{mn} = 0\}$ and $W_{mn} = \{x_m < \infty \text{ and } z_{mn} = 1\}$. Assuming the independence of the random variables x_m (consistent with the locally tree-like assumption used in the previous section), we can rewrite Eq. (3.2) as

$$\phi_n(s) = e^{-s} \prod_m E\Big[e^{-sz_{mn}x_m} | Z_{mn} \cup W_{mn}\Big], \tag{3.3}$$

where the expectation $E[\cdot]$ is taken over realizations of the random pairs (z_{mn}, x_m). Denoting by $P(W)$ the probability of an event set W, we relate the expected value in the product in Eq. (3.3) to the probabilities of the events W_{mn} and Z_{mn}:

$$\begin{aligned} &E[e^{-sz_{mn}x_m} | Z_{mn} \cup W_{mn}] P(Z_{mn} \cup W_{mn}) \\ &\quad = E[e^{-sz_{mn}x_m} | Z_{mn}] P(Z_{mn}) + E[e^{-sz_{mn}x_m} | W_{mn}] P(W_{mn}). \end{aligned} \tag{3.4}$$

Using the following relations that follow from the definitions above,

$$\begin{aligned} P(Z_{mn}) &= 1 - A_{mn}, \\ P(W_{mn}) &= A_{mn} b_m, \\ P(Z_{mn} \cup W_{mn}) &= (1 - A_{mn}) + A_{mn} b_m, \\ E[e^{-sz_{mn}x_m} | W_{mn}] &= \phi_m(s), \\ E[e^{-sz_{mn}x_m} | Z_{mn}] &= 1, \end{aligned}$$

Eq. (3.4) gives

$$E[e^{-sz_{mn}x_m} | Z_{mn} \cup W_{mn}] = \frac{(1 - A_{mn}) + b_m A_{mn} \phi_m(s)}{(1 - A_{mn}) + b_m A_{mn}}. \tag{3.5}$$

Inserting this into Eq. (3.3) we obtain one of our main results:

$$\phi_n(s) = e^{-s} \prod_m \frac{(1 - A_{mn}) + b_m A_{mn} \phi_m(s)}{(1 - A_{mn}) + b_m A_{mn}}. \tag{3.6}$$

Defining $g_n(s) = \phi_n(s) - 1$, and the matrix H with entries

$$H_{mn} = \frac{b_m A_{mn}}{(1 - A_{mn}) + b_m A_{mn}}, \tag{3.7}$$

we can rewrite this equation as

$$1 + g_n(s) = e^{-s} \prod_m [1 + H_{mn} g_m(s)]. \tag{3.8}$$

Defining the $N \times N$ matrix, $B = \text{diag}(b_1, b_2, ..., b_N)$, we have from Eqs. (2.15) and (3.7), that $HB^{-1} = B^{-1}D$. Thus the matrix H is related to the matrix D by a similarity transformation and thus has the same spectrum. Therefore, we will denote the Perron-Frobenius eigenvalue of H by λ_D. Note that $\lambda_D = \lambda$ when $\lambda \leq 1$, since in that case $b_n = 1$ and $H = D = A$.

Next we present two methods for finding information about the distribution of sizes x_n from the moment generating function. The methods are consistent with each other, but both are presented in order to provide another method to numerically verify our results. The first is the "brute force" method of numerically taking successive derivatives of the moment generating function and evaluating at $s = 0$ to find each moment. A second method involves approximating time as a continuous variable and taking the inverse Laplace transform. It is demonstrated specifically for critical networks using Post's inversion formula, then again through an asymptotic argument.

3.1 "Brute Force" Method

We start by taking the natural log of Eq. (3.8), and expanding the product as a sum to obtain

$$\ln [1 + g_n(s)] = -s + \sum_m \ln [1 + H_{mn} g_m(s)]. \tag{3.9}$$

Expanding the natural logs in series and solving for s, we find

$$s = \sum_{m=1}^{N} H_{mn} g_m - g_n + \frac{1}{2}\Big[g_n^2 - \sum_{m=1}^{N} H_{mn}^2 g_m^2\Big] + O(g_n^3). \tag{3.10}$$

By matching leading order terms as $s \to 0$ we can describe the behavior of g_n. We thoroughly examine three possibilities below: (a) $g_n/s \to 0$, (b) $s/g_n \to 0$, and (c) $g_n \sim s$.

(a) $s/g_n \to 0$ implies that for (3.10) to balance as $s \to 0$,

$$0 = \sum_{m=1}^{N} H_{mn} g_m - g_n \tag{3.11}$$

and so $H^T \mathbf{g} = \mathbf{g}$. This implies that $\mathbf{g}$ is the left Perron-Frobenius eigenvector of A corresponding to eigenvalue $\lambda_D = 1$, and since $\lambda_D = 1$ only when $\lambda = 1$ (proved below), $s/g_n \to 0$ is only possible if the network is critical. Balancing the second order terms implies $g_n^2 \sim s$ and therefore $g_n \sim s^{1/2}$.

(b) $g_n/s \to 0$ is impossible because it leaves the left- and right-hand sides of (3.10) asymptotically unbalanced as $s \to 0$.

(c) $g \sim s$ implies that for (3.10) to balance as $s \to 0$,

$$s = \sum_{m=1}^{N} H_{mn} g_m - g_n \tag{3.12}$$

For the sake of contradiction, assume that $\lambda = 1$, rewriting Eq. (3.12) as

$$(H^T - I)\mathbf{g} = s\mathbf{1}, \tag{3.13}$$

Then left multiplying Eq. (3.13) by the eigenvector corresponding to $\lambda = 1$ we find

$$\begin{aligned} (1-1)u^T \mathbf{g} &= s u^T \mathbf{1} \\ 0 &= s \sum_{m=1}^{N} u_m \end{aligned} \tag{3.14}$$

which clearly leads to a contradiction, since $\mathbf{u}$ is the Perron-Frobenius eigenvector of A, and therefore all of its entries are positive so $\sum u_m > 0$. Therefore, if $g_n \sim s$ then the network cannot be critical.

Together, the analysis of (a), (b), and (c) above imply that if a network is critical, $g_n \sim s^{1/2}$ and if a network is subcritical or supercritical, $g_n \sim s$. We invoke Post's inversion formula,

$$f(t) = \lim_{k\to\infty} \frac{(-1)^k}{k!}\Big(\frac{k}{t}\Big)^{k+1} F^{(k)}\Big(\frac{k}{t}\Big) \tag{3.15}$$

We can use Post's inversion forumla to take the inverse transformation of $F(t) = 1 - s^\alpha$ with $\alpha < 1$, where we are particularly interested in $\alpha = 1/2$. Since α is not an integer the kth derivative is given by

$$F^{(k)}(s) = -(\alpha)(\alpha-1)\dots(\alpha-k+1)s^{\alpha-k} \tag{3.16}$$

$$= (-1)^k(\alpha)\Big[(1-\alpha)(2-\alpha)...(k-\alpha-1)\Big]s^{\alpha-k} \tag{3.17}$$

$$= (-1)^k\alpha\frac{\Gamma(k-\alpha)}{\Gamma(1-\alpha)}s^{\alpha-k} \tag{3.18}$$

Inserting $F^{(k)}$ into (3.15) we get

$$f(t) = \lim_{k\to\infty} \frac{(-1)^k}{k!}\Big(\frac{k}{t}\Big)^{k+1}\Big(\frac{k}{t}\Big)^{\alpha-k}(-1)^k\alpha\frac{\Gamma(k-\alpha)}{\Gamma(1-\alpha)} \tag{3.19}$$

$$= \lim_{k\to\infty} \frac{\alpha}{k!}\Big(\frac{k}{t}\Big)^{\alpha+1}\frac{\Gamma(k-\alpha)}{\Gamma(\alpha-1)} \tag{3.20}$$

Then using $k! = k\Gamma(k)$ and Stirling's formula for $k!$, $k! \approx \sqrt{2\pi}n^{n+1/2}e^{-n}$ we find

$$f(t) = \frac{\alpha}{\Gamma(1-\alpha)}t^{-1-\alpha}\lim_{k\to\infty} k^\alpha\frac{k}{k-\alpha+1}\frac{\Gamma(k-\alpha)}{\Gamma(k+1)} \tag{3.21}$$

$$= \frac{\alpha}{\Gamma(1-\alpha)}t^{-1-\alpha}\lim_{k\to\infty} e^\alpha\Big(\frac{k-\alpha}{k}\Big)^{k-\alpha+1/2} \tag{3.22}$$

$$= \frac{\alpha}{\Gamma(1-\alpha)}t^{-1-\alpha} \tag{3.23}$$

So for the critical case when $F(s) \sim 1 - s^\alpha$ then $f(t) \sim t^{-1-\alpha}$. We showed in 3.1 that $\alpha = 1/2$. So we

can conclude that

$$P(x) \approx \frac{k}{2\Gamma(1/2)} x^{-3/2} \tag{3.24}$$

which is the probability that an avalanche will have size x in a critical network.

Eq. (3.24) constitutes our main prediction of avalanche size distribution, applicable only to critical networks. For subcritical and supercritical networks, one is tempted to guess that, just as in the analysis for duration, the distributions for non-critical size will be exponential. Furthermore if we suppose that the probability density function for avalanche size is an exponential with rate α, its moment generating function is $\phi(s) = \alpha/(\alpha + s)$, which expanded to leading order is $\phi(s) \approx 1 - \frac{s}{\alpha}$, making the argument even more tempting. However, if the Laplace transform of an exponential, $\phi(s) = \alpha/(\alpha + s)$ is used as an ansatz to solve Eq. (3.3), one notices immediately that the right-hand side cannot equal the left-hand side due to an imbalance in the order of the poles at $s = -\alpha$. Therefore we conclude that the distribution of sizes does not follow an exponential distribution. An investigation of what type of distribution occurs in the subcritical and supercritical cases will be deferred until the next section

Recall that expanding the moment generating function yields

$$\phi_n(s) = E[e^{-sX_n}|X_n \text{ is finite}] = 1 - sE[X_n|X_n \text{ is finite}] + s^2 E[X_n^2|X_n \text{ is finite}]/2 - ... \tag{3.25}$$

which allows us to numerically calculate the moments $\phi(0) = 1, \phi'(0) = -E[X_n|X_n \text{ is finite}]$... etc. provided that the moments are finite. If we let $\phi'(0) = [\phi_1'(0), \phi_2'(0), ..., \phi_N'(0)]^T$. From Eq. (3.1) we differentiate and evaluate at $s = 0$ and solve,

$$\phi_n'(0) = -1 + \sum_{m=1}^{N} A_{mn}\phi_m'(0) \tag{3.26}$$

$$\phi'(0) = -(I - A^T)^{-1}\overrightarrow{1}. \tag{3.27}$$

Similarly, by differentiating twice and evaluating at 0 we find

$$(I - A^T)\phi''(0) = -\phi'(0) + \phi'(0)A\phi'(0) - A^{(2)}\phi'(0) \tag{3.28}$$

where $A^{(2)}$ is a matrix whose entries are the entries of A squared elementwise. Using these two formulas we may numerically find the mean and variance of the distribution of avalanche size.

3.2 Inverting The Laplace Transform

The asymptotic form for the distribution of the sizes of avalanches starting at node n, $p_n(x)$, can be obtained from the asymptotic form of $g_n(s)$ as $s \to 0$. Therefore, we study Eq. (3.8) by assuming $g_n(s)$ is small. In order to obtain an analytic expression for the distribution of sizes we assume, in addition, that the network is close to critical, $(\lambda_D - 1) \ll 1$. Taking logarithms in Eq. (3.8) and using the approximation $\ln(1+g) \approx g - g^2/2$ we obtain

$$g_n(s) - \frac{1}{2}g_n(s)^2 = -s + \sum_m H_{mn}g_m(s) - \frac{1}{2}\sum_m H_{mn}^2 g_m^2(s). \tag{3.29}$$

As $s \to 0$ and $g_n \to 0$, the leading order terms are $g_n(s) = -s + \sum_m H_{mn}g_m(s)$, or $(H^T - I)\mathbf{g} = s\mathbf{1}$, where $\mathbf{g} = [g_1, g_2, \ldots, g_N]^T$ and $\mathbf{1} = [1, 1, \ldots, 1]^T$. When $|\lambda_D - 1| \ll 1$, and λ_D is well separated from the rest of the spectrum of H as is the case in networks without strong community structure [29], $\mathbf{g} = s(H^T - I)^{-1}\mathbf{1} \sim \mathbf{v}$, where $\mathbf{v}$ is the left Perron-Frobenius eigenvalue of H. Since $\mathbf{v}$ is independent of s, the solution up to first order is approximately $g_n(s) = g(s)v_n/\langle v\rangle$, where the term $\langle v\rangle = \frac{1}{N}\sum_{n=1}^{N} v_n$ is included to make $g(s)$ independent of the normalization of $\mathbf{v}$. For small s, and including the nonlinear terms, we expect the solution of Eq. (3.29) to be close to the first-order solution, so we set

$$g_n(s) = g(s)\langle v\rangle^{-1}v_n + \varepsilon_n(s) \tag{3.30}$$

where ε_n is a small unkown error term. Substituting Eq. (3.30) into Eq. (3.29), using $H^T\mathbf{v} = \lambda_D\mathbf{v}$, and

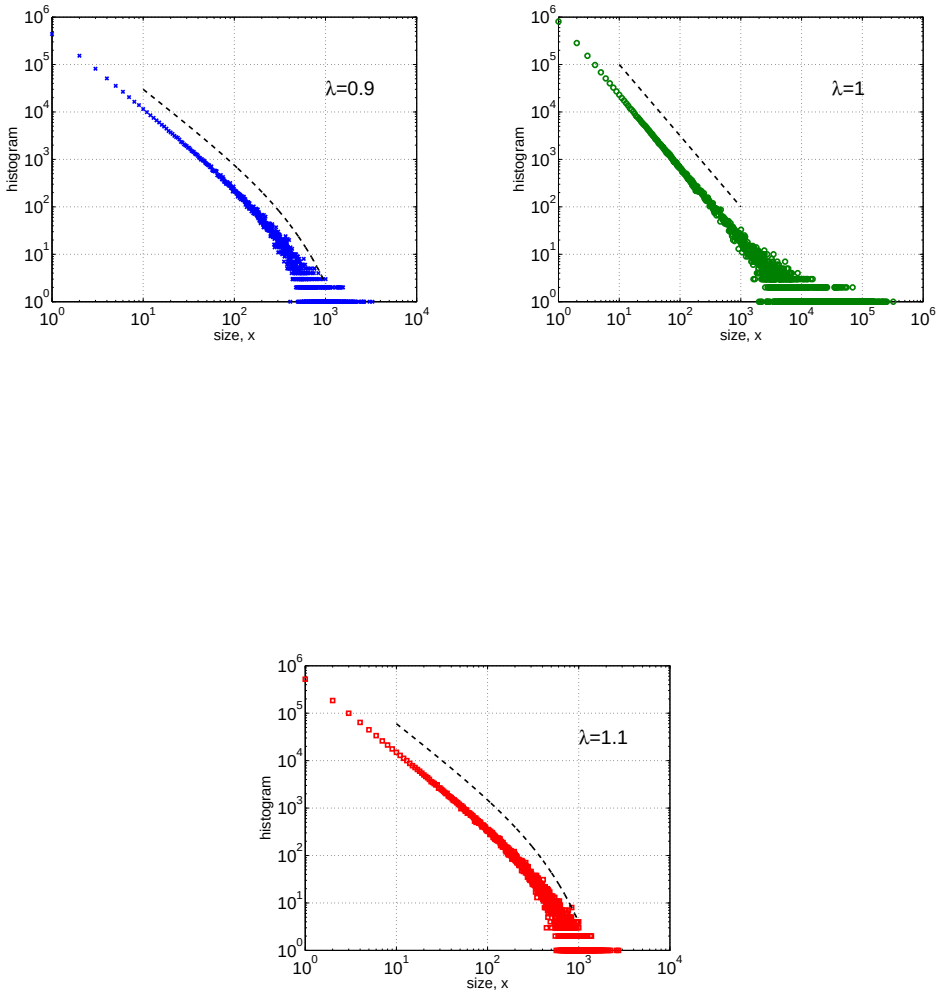

Figure 3.1: Histograms of avalanche sizes shown above for networks of $N = 10^5$ nodes with power law degree distribution, exponent $\gamma = 3.5$ with Perron-Frobenius eigenvalues of $\lambda = 0.9$ (top left), $\lambda = 1.0$ (top right) and $\lambda = 1.1$ (bottom) on a log-log scale. Data are the exact recorded histograms from a single simulation of 10^6, $2 \cdot 10^6$, and 10^6 avalanches respectively from left to right. Dashed lines provide a reference for the theoretical prediction $x^{-3/2} \exp(-x/x^*)$ described in Eqs. (3.37) and (3.38). Infinite size avalanches in the supercritical case (bottom) are not represented in the data set. Agreement between theoretical prediction and measurement is excellent despite finite sample size noise.

neglecting terms of order εg we get

$$\begin{aligned} & g(s)\langle v\rangle^{-1}v_n + \varepsilon_n(s) - \frac{1}{2}g(s)^2\langle v\rangle^{-2}v_n^2 \\ & = -s + \lambda g(s)\langle v\rangle^{-1}v_n + \sum_m H_{mn}\varepsilon_m(s) - g(s)^2\langle v\rangle^{-2}\frac{1}{2}\sum_m H_{mn}^2 v_m^2. \end{aligned} \tag{3.31}$$

To eliminate the unknown error term ε_n, we multiply by the right eigenvector entry u_n of H and sum over n. We use $H\mathbf{u} = \lambda_D\mathbf{u}$ and neglect $(\lambda - 1)\varepsilon_n$ to get

$$\begin{aligned} & g(s)\langle v\rangle^{-1}\langle uv\rangle - \frac{1}{2}g(s)^2\langle v\rangle^{-2}\langle uv^2\rangle \\ & = -s\langle u\rangle + \lambda_D g(s)\langle v\rangle^{-1}\langle uv - g(s)^2\langle v\rangle^{-2}\frac{1}{2N}\sum_n\sum_m u_n H_{mn}^2 v_m^2, \end{aligned} \tag{3.32}$$

where $\langle xy\rangle \equiv \frac{1}{N}\sum_n x_n y_n$. Eq. (3.32) is a quadratic equation for $g(s)$, $ag^2 + bg + c = 0$, with

$$a = \frac{\sum_n\sum_m u_n(1 - H_{mn}^2)v_m^2}{2N\langle uv\rangle\langle v\rangle}, \tag{3.33}$$

$$b = (\lambda_D - 1), \tag{3.34}$$

$$c = -s\frac{\langle u\rangle\langle v\rangle}{\langle uv\rangle}. \tag{3.35}$$

Solving for $g(s)$ and substituting back into $g_n(s) = \phi_n(s) - 1$ we find, choosing the root that guarantees $g_n < 0$,

$$\phi_n(s) = 1 + \frac{-(\lambda_D - 1) - \sqrt{(\lambda_D - 1)^2 + 4sa\frac{\langle u\rangle\langle v\rangle}{\langle uv\rangle}}}{2a}\frac{v_n}{\langle v\rangle} \tag{3.36}$$

The moment generating function in Eq. (3.2) can be interpreted as the Laplace transform of the distribution of sizes, if the sizes are approximated by a continuous variable. Taking the inverse Laplace transform of $\phi_n(s)$ in Eq. (3.36) we obtain that for large x, the distribution of sizes $p_n(x)$ is approximately given by

$$p_n(x) \propto x^{-3/2}\exp(-x/x^*)v_n, \tag{3.37}$$

where the characteristic size x^* is given by

$$x^* = 4a\frac{\langle v\rangle\langle u\rangle}{\langle vu\rangle}(\lambda_D - 1)^{-2}. \tag{3.38}$$

The distribution of sizes is asymptotically an exponential times a power-law with exponent $-3/2$. In the critical case, when $\lambda = \lambda_D = 1$, x^* diverges and we recover a power law distribution with exponent $-3/2$, which is the well known exponent for critical branching processes [4]. It is interesting to note that this exponent, in our model, does not depend on the structure of the network, as opposed to related percolation models where all nodes with the same degree are considered statistically equivalent [5]. Also note that the quantity a in Eq. (3.38) depends implicitly on λ_D.

3.3 Numerical Verification

In Fig. 3.1 we compare histograms of avalanche sizes obtained from direct numerical simulations (colored symbols) for $\lambda = 0.9$, 1.0, and 1.1 with our theoretical predictions described in the previous paragraph (dashed lines). Note that, since our predictions allow for an unspecified proportionality constant, the vertical position of the dashed lines was chosen arbitrarily. In general, we find excellent agreement between the theoretical predictions of avalanche duration and size distributions with the histograms observed in experiment. While the dashed lines in Fig. 3.1 are appealing to the eye, quantitative measures of agreement between theory and experiment are shown in Fig. 3.3.

As a partial test of our theory for the distribution of avalanche sizes, the distribution is assumed to be of the form $x^{-3/2}\exp(-x/x^*)$, and x^* is estimated from the data, which is then compared with our theoretical prediction in Eq. (3.38). Note that a stronger test, which we did not pursue, would be to validate the model $x^{-\gamma}\exp(-x/x^*)$ using statistical tests. Noting that since x^* will diverge as $\lambda \to 1$, $1/x^*$ was estimated via a nonlinear least-squares using Brent's minimization on the cumulative histogram of the avalanche size data. Since our theory describes only the asymptotic form of the distribution, this estimate was performed only on the largest 10% of measured data [similar results were obtained using the largest 5%, 1% and 0.1% of data (not shown), but when using more than the largest 10% the minimizing x^* value

diverged, suggesting that we fit the power-law portion of data at the expense of the exponential tail]. Fig. 3.3 shows our theoretical prediction (solid red line) and the result of the numerical fit to the data (circles; the lines are to aid the eye). As shown, agreement is quite good close to $\lambda_D = 1$ (see the inset of Fig. 3.3), but less accurate for very subcritical or supercritical networks, which is consistent with the assumption that $|\lambda_D - 1|$ is a small quantity which was used in the derivation of Eq. (3.38).

Although Figs. 2.3 and 3.3 demonstrate agreement between theory and measurement for supercritical networks, that analysis was restricted to finite avalanches. To complement this result, we compare the predicted fraction of infinite avalanches with the measured fraction, for various values of λ_D. The quantity b_n in Eq. (2.3) is the fraction of avalanches originating at node n which will have finite duration and size. In Fig. 2.1, we show the fraction of avalanches that decay in finite time, averaged over nodes, comparing theory (solid line) with experiment (circles). The theoretical fraction of avalanches is calculated by numerically solving equation Eq. (2.3) to find $b_n, n = 1 \ldots, N$, and then plotting $\sum_{n=1}^{N} b_n/N$ as a function of λ. The numerical fraction of finite avalanches was calculated by simulating 10^6 avalanches, each one starting at a random node (out of $N = 10^5$ total nodes). If an avalanche lasted more than 10^6 steps, we counted it as an infinite avalanche. Then, an estimate of b_n, $\hat{b}_n$, was calculated as the fraction of finite avalanches starting at node n. The symbols in Fig. 2.1 show $\sum_{n=1}^{N} \hat{b}_n/N$ as a function of λ. We note that, although there are relatively few avalanches per node, the large number of nodes averages out the errors incurred in estimating individual b_n from such a small sample. Agreement is excellent over the entire range of λ values tested.

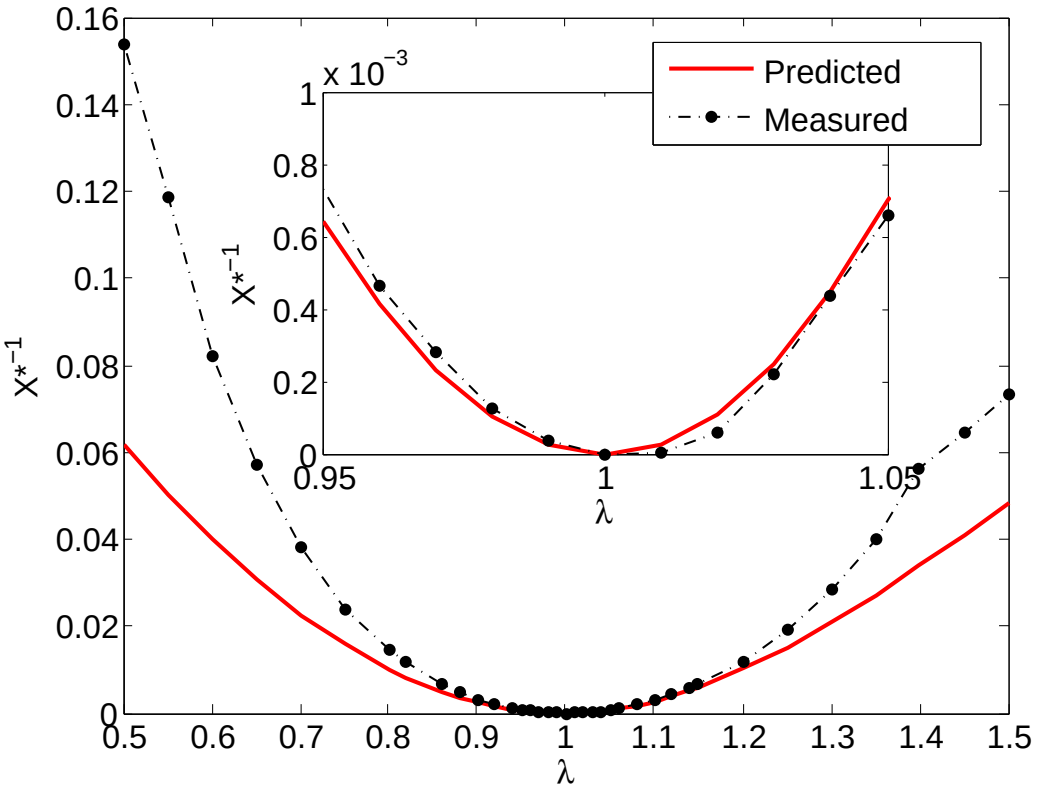

Figure 3.2: Testing the prediction that avalanche size x is distributed as $x^{-3/2}\exp(-x/x^*)$, we compare the theoretical prediction of x^* (red solid line) with x^* estimated via regression on the largest 10% of avalanches from numerical simulations (black points, dashed line). Inset, identical data on a magnified domain around $\lambda = 1$. Agreement is excellent for λ near 1, and decreasingly accurate for much larger or smaller λ.

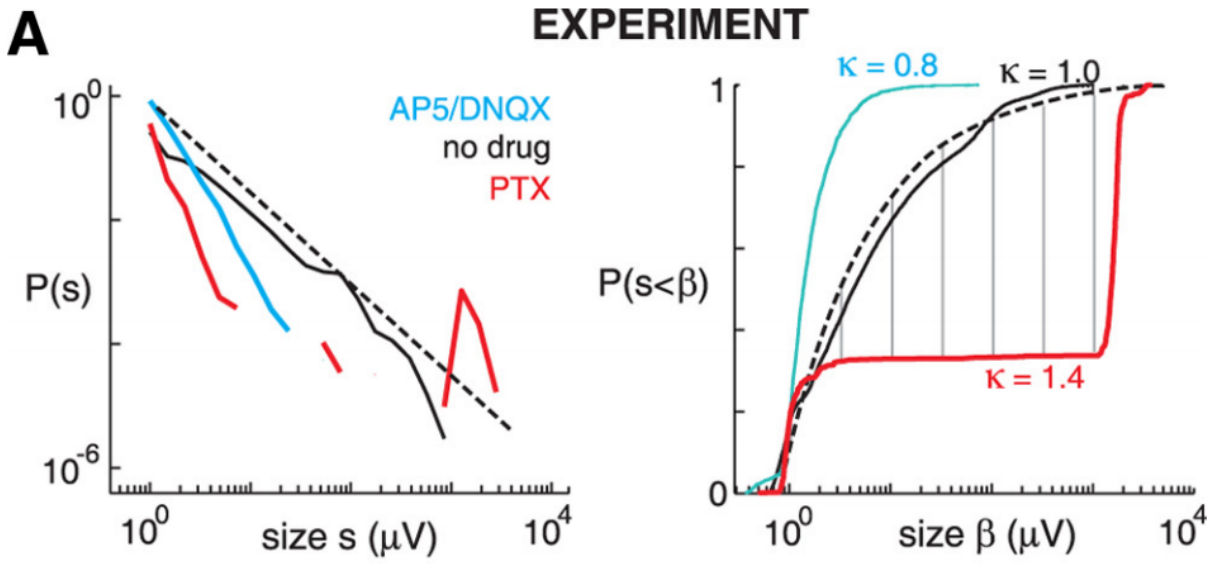

Figure 3.3: From [11], Data is taken on size of cortical avalanches from the brain of a rat. The left graph shows the PDF of avalanche sizes while the right one shows the CDF. The black line is for a typical rat cortex, the blue line is measured from cells who have been treated with AP5/DNQX which is a drug that enhances inhibition, and the red line is treated with PTX which is a drug that enhances excitation. These are biologically analagous to critical (black), subcritical (blue), and supercritical (red) networks and their size distributions.

Chapter 4

Discussion

We have presented an analysis of the asymptotic distributions of the duration and sizes of avalanches in complex networks. This work is of interest in various applications, most notably neuroscience [11, 16, 18, 10] and the analysis of power-grid failure cascades [34]. While some of our results, such as the functional forms for the distributions, are analogous to those found in classical Galton-Watson branching processes [2] or in mean-field models [5], we emphasize the distinguishing aspects of our results: (i) We generalize the criterion for criticality to $\lambda = 1$, which depends on the topology of the network in ways that previous mean-field results do not capture; (ii) The parameters of the asymptotic distributions in the various regimes are affected by the network topology, and our results allow us to predict how various factors (e.g., network degree distributions, degree-degree correlations) affect these parameters [e.g., the parameter x^* in Eq. (3.38) or λ_D in Eq. (2.17)]. (iii) In contrast to previous studies, our results allow us to predict the statistics of avalanches generated at a particular node. This might be of critical importance in certain applications where the adjacency matrix is known or can be inferred (such as the power grid or the Autonomous System network of the internet) since one can then allocate resources to prevent avalanches, if so desired, that start at the nodes which tend to generate the largest avalanches. As shown in Fig. 2.4, the naive prediction that the nodes with the largest out-degree generate the largest avalanches is not necessarily true when the networks have nontrivial structure, such as degree-degree correlations.

In developing our theory, we made some assumptions which we now discuss. First, we assumed that the network was locally tree-like. This allowed us to treat avalanches propagating to the neighbors of a given node as independent of each other. While this is a good approximation for the networks we used, it is

certainly not true in general. In particular, avalanches propagating separately from a given node might excite the same node as they grow. The result is that the number of nodes that the avalanches excite in simulation may be less than what the theory would predict. In running our simulations, we addressed this issue in two ways: first, we kept track of the number of times two branches of the same avalanche simultaneously excited the same node n, finding it to be an increasing function of avalanche size and Perron-Frobenius eigenvalue, yet still negligible when compared to the total number of excitations. In addition, each time such an event occurred, we separately generated an avalanche starting from the doubly excited node n and corrected both the size and duration of the original avalanche by incorporating these additional avalanches. We found that doing this had no appreciable effect on the measured distributions. All figures shown in this manuscript are produced from simulation data *without* the additional compensating avalanches included. This, and the fact that the numerical simulations are described well by the theory, suggest that the interaction of avalanches propagating to different neighbor nodes can be safely neglected in the networks studied. The performance of our theory in networks that are not locally tree-like, such as networks with a high degree of clustering, is left for future research. Another approximation we used is that the Perron-Frobenius eigenvalue λ is well separated from the rest of the spectrum. This is a good approximation in networks without well defined communities, but can break down in networks with strong community structure [29].

Finally, we note that our results show that the experimental signatures of criticality in neural systems (characterized by a power-law distribution of avalanche sizes and durations with exponents $-3/2$ and -2, respectively [18, 11, 10, 16]) are robust to complex underlying network topologies.

Bibliography

[1] Henry W. Watson and Francis Galton. On the probability of the extinction of families. Journal of the Anthropological Institute of Great Britain, 4:138–144, 1875.

[2] Theodore E. Harris. The Theory of Branching Processes. Dover Publications, New York, 1963.

[3] Krishna B. Athreya and Peter E. Ney. Branching Processes. Springer Verlag, Berlin, 1972.

[4] Deokjae S. Lee, Kwang I. Goh, Byungnam Kahng, and Dohun Kim. Branching process approach to avalanche dynamics on complex networks. Journal of the Korean Physical Society, 44:633–637, 2004.

[5] Rueven Cohen, Daniel ben Avraham, and Shlomo Havlin. Percolation critical exponents in scale-free networks. Physical Review E, 66:036113, 2002.

[6] Adam Hackett, Sergey Melnik, and James P. Gleeson. Cascades on a class of clustered random networks. Physical Review E, 83:056107, 2011.

[7] Björn Samuelsson and Joshua E.S. Socolar. Exhaustive percolation on random networks. Physical Review E, 74:036113, 2006.

[8] James P. Gleeson. Mean size of avalanches on directed random networks with arbitrary degree distributions. Physical Review E, 77:057101, 2008.

[9] Marc Benayoun, Jack D. Cowan, Wim van Drongelen, and Edward Wallace. Avalanches in a stochastic model of spiking neurons. Public Library of Science Computational Biology, 6:e1000846, 2010.

[10] Thomas Petermann, Tara C. Thiagarajan, Mikhail Lebedev, Miguel Nicolelis, Dante R. Chialvo, and Dietmar Plenz. Spontaneous cortical activity in awake monkeys composed of neuronal avalanches. Proceedings to the National Academy of Science, 106:15921–15926, 2009.

[11] Woodrow L. Shew, Hongdian Yang, Thomas Petermann, Rajarshi Roy, and Dietmar Plenz. Spontaneous cortical activity in awake monkeys composed of neuronal avalanches. Journal of Neuroscience, 29:15595–15600, 2009.

[12] Craig V. Stewart and Dietmar Plenz. Homeostasis of neuronal avalanches during postnatal cortex development in vitro. Journal of Neuroscience, 169:405–416, 2008.

[13] Daniel B. Larremore, Woodrow L. Shew, and Juan G. Restrepo. Predicting criticality and dynamic range in complex networks: Effects on topology. Physical Review Letters, 106:058101, 2011.

[14] Daniel B. Larremore, Woodrow L. Shew, Edward Ott, and Juan G. Restrepo. Effects of network topology, transmission delays, and refractoriness on the response of coupled excitable systems to a stochastic stimulus. Chaos, 21:025117, 2011.

[15] Osame Kinouchi and Mauro Copelli. Optimal dynamical range of excitable networks at criticality. Nature Physics, 2:348–351, 2006.

[16] Woodrow L. Shew, Hongdian Yang, Shan Yu, Rajarshi Roy, and Dietmar Plenz. Information capacity and transmission are maximized in balanced cortical networks with neuronal avalanches. Journal of Neuroscience, 31:55–63, 2011.

[17] Takuma Tanaka, Takeshi Kaneko, and Toshio Aoyagi. Recurrent infomax generates cell assemblies, neuronal avalanches, and simple cell-like selectivity. Neural Computation, 21:1038–1067, 2009.

[18] John M. Beggs and Dietmar Plenz. Neuronal avalanches in neocortical circuits. Journal of Neuroscience, 23:11167–11177, 2003.

[19] Juan G. Restrepo. Class notes for appm 7400, dynamics on networks. Technical report, Department of Applied Mathematics, University of Colorado-Boulder, August.

[20] Charles R. MacCluer. The many proofs and applications of perron's theorem. SIAM Review, 42:487–498, 2000.

[21] Albert L. Barabási and Réka Albert. Emergence of scaling in random networks. Science, 286:509–512, 1999.

[22] Melvyn. Goldstein, Steven A. Morris, and Gary G. Yen. Problems with fitting to the power-law distribution. The European Physical Journal B - Condensed Matter and Complex Systems, 41:255–258, 2004.

[23] Mark E.J. Newman. Assortative mixing in networks. Physical Review Letters, 89:208701, 2002.

[24] Juan G. Restrepo, Edward Ott, and Brian R. Hunt. Approximating the largest eigenvalue of network adjacency matrices. Physical Review E, 76:056119, 2007.

[25] Mark E.J. Newman. The structure and function of complex networks. SIAM Review, 45:167–256, 2003.

[26] Sergey Melnik, Adam Hacket, Mason A. Porter, Peter J. Mucha, and James P. Gleeson. The unreasonable effectiveness of tree-based theory for networks with clustering. Physical Review E, 83:036116, 2011.

[27] Juan G. Restrepo, Edward Ott, and Brian R. Hunt. Characterizing the dynamical importance of network nodes and links. Physical Review Letters, 97:094102, 2006.

[28] Andrew Pomerance, Edward Ott, Michelle Girvan, and Wolfgang Losert. The effect of network topology on the stability of discrete state models of genetic control. Proceedings to the National Academy of Science, 106:8209–8214, 2009.

[29] Sanjeev Chauhan, Michelle Girvan, and Edward Ott. Spectral properties of networks with community structure. Physical Review E, 80:056114, 2009.

[30] Paul Erdős and Tibor Gallai. Graphs with prescribed degrees of vertices. Matematikai Lapok, 11:166–177, 1960.

[31] Tom Britton, Maria Deijfen, and Anders Martin-Löf. Generating simple random graphs with prescribed degree distribution. Journal of Statistical Physics, 124:1377–1397, 2006.

[32] Mark E.J. Newman. Mixing patterns in networks. Physical Review E, 67:026126, 2003.

[33] Paul Erdős and Alfréd Rényi. On random graphs. Publicationes Mathematicae Debrecen, 6:290–297, 1959.

[34] Réka Albert, István Albert, and Gary L. Nakarado. Structural vulnerability of the north american power grid. Physical Review E, 69:025103, 2004.

[35] Henrik J. Jensen. Self-Organized Criticality: Emergent Complex Behavior in Physical and Biological Systems. Cambridge University Press, Cambridge, 1998.

[36] Krishna B. Athreya. On the absolute continuity of the limit random variable in the supercritical galton-watson branching process. Proceedings to the American Mathematical Society, 30:563–565, 1971.

[37] Stefano Zapperi, Kent B. Lauritsen, and H. Eugene Stanley. Self-organized branching processes: Mean field theory for avalanches. Physical Review Letters, 75:4071–4074, 1995.

[38] Russell Lyons and Yuval Peres. Probability on trees and networks. 1988.

[39] Antoine Allard, Pierre-André Noel, Louis J. Dube, and Babak Pourbohloul. Heterogeneous bond percolation on multitype networks with an application to epidemic dynamics. Physical Review E, 79:036113, 2009.

[40] Joel C. Miller. Percolation and epidemics in random clustered networks. Physical Review E, 80:020901, 2009.

[41] Erik Volz. SIR dynamics in random networks with heterogeneous connectivity. Journal of Mathematical Biology, 56:293–310, 2008.

[42] Mark E.J. Newman. Networks: An Introduction. Oxford University Press, Oxford, 2010.